Particle Detectors

Lecture 8
06/04/18

a.a. 2017-2018

Emanuele Fiandrini

All transparent materials are candidates for Cherenkov radiators. In particular, Cherenkov radiation is emitted in all scintillators and in the light guides which are used for the readout.

The threshold counter has only one adjustable parameter, the refractive index of the radiator. To control the threshold you must control the refractive index (e.g., vary the pressure in a gas filled counter). In fig. are shown the appropriate refractive indices for pions and kaons of varying momentum.

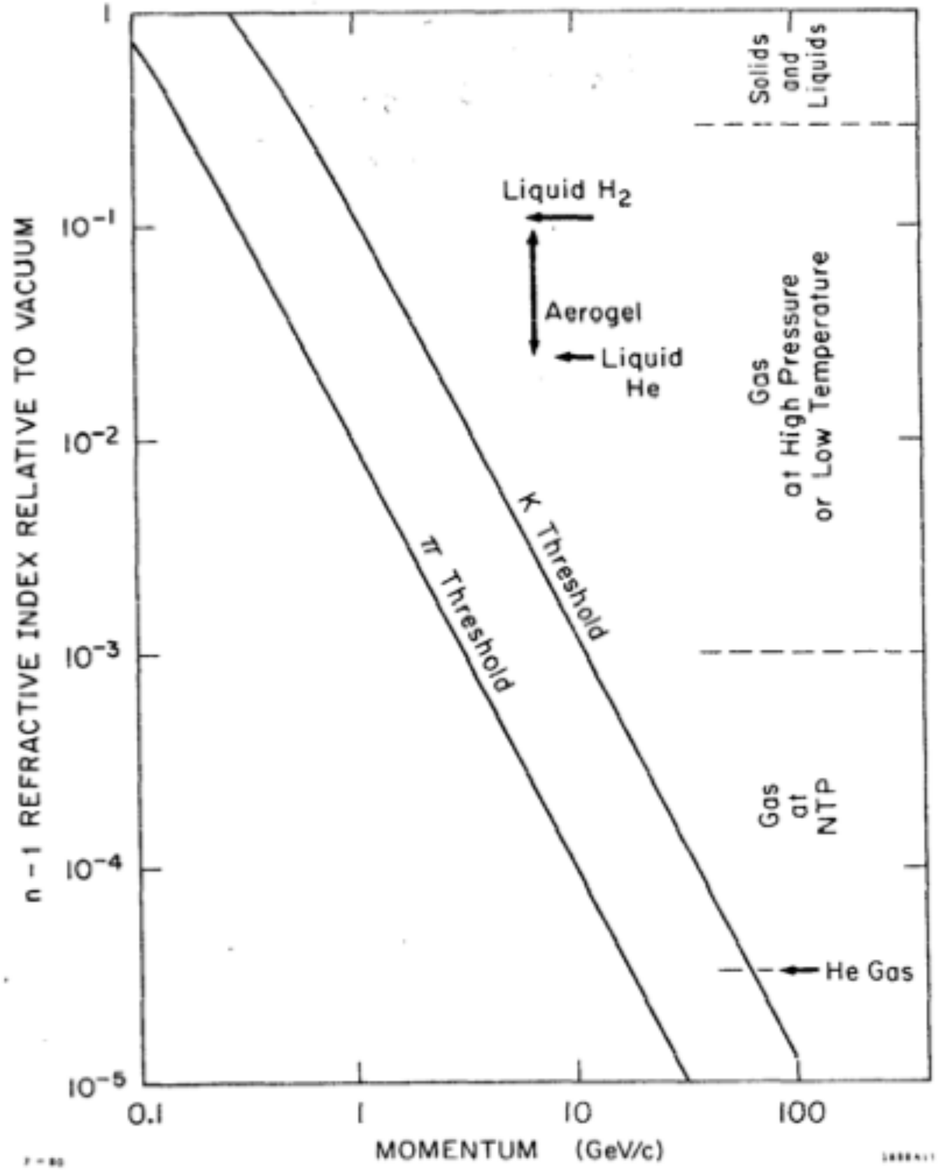

Fig. 4. The refractive index required so that of pions or kaons of given momentum be at threshold for Čerenkov radiation.

Types of Cerenkov Counters

Differential Cerenkov Counter:
Makes use of the angle of Cerenkov radiation and only samples light at certain angles.
For fixed momentum $\cos\theta$ is a function of mass:

$$\cos\theta = \frac{1}{n\beta} = \frac{1}{n(p/E)} = \frac{\sqrt{m^2 + p^2}}{np}$$

Differential cerenkov counters typically on work over a fixed momentum range (good for beam monitors, e.g. measure π or K content of beam).
Problems with differential Cerenkov counters:
  Optics are usually complicated.
  Have problems in magnetic fields since phototubes must be shielded from B-fields above a few tenths of a gauss.

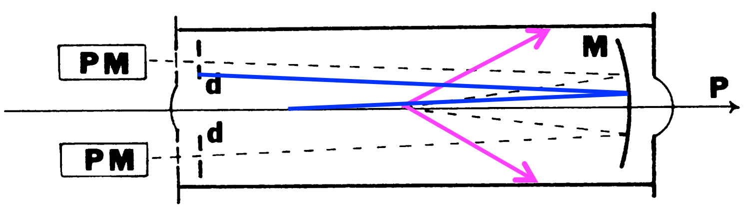

Not all light will make it to phototube

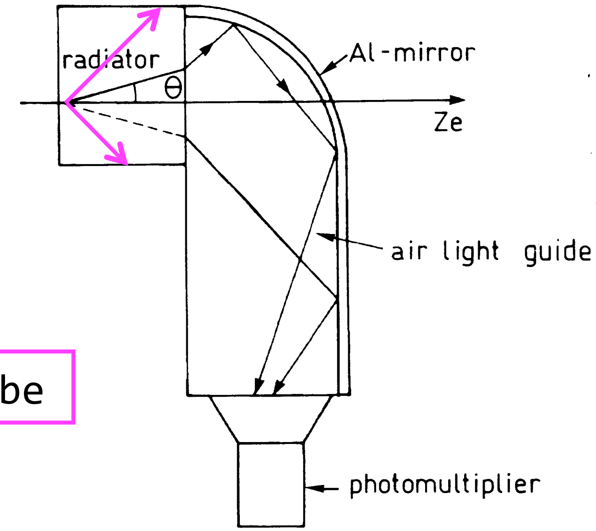

Differential Detectors

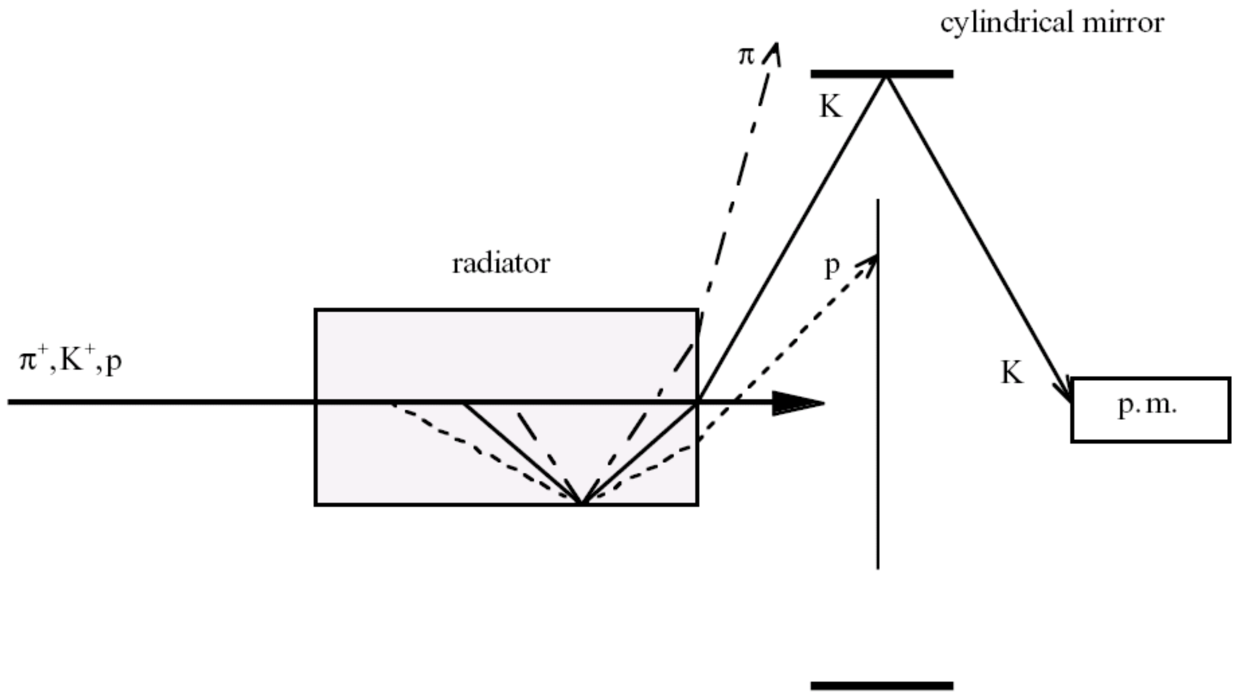

- Will reflect light onto PMT for certain angles only ⇔ β Selection

Ring Imaging Cherenkov Counters (RICH)

RICH counters measure the cone angle θ_c of the Cerenkov light by projecting it on a photon-sensitive plane.

By measuring θ_c, one measures β.

The ½ angle (θ) of the cone is given by: $\cos\theta = \dfrac{1}{n\beta}$

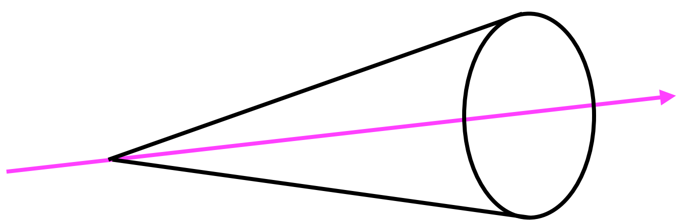

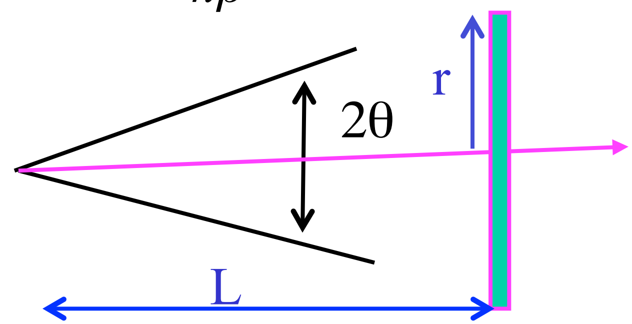

The radius of the cone is: **r=Ltanθ**, with L the distance to the where the ring is imaged.

Since one is not only interested in detecting photons, but also in measuring their coordinates, a position-sensitive detector is necessary.

Problems with RICH:
- optics can be very complicated (projections are not usually circles)
- readout system very complicated (e.g. wire chamber readout, 10^5-10^6 channels)
- photon yield usually small (10-20), only a few points on "circle"

Ring Imaging Detectors

If the momentum of the charged particle is already known, e.g. by magnetic deflection, then the particle can be identified (i.e. its mass m determined) from the size of the Cherenkov ring, r.
By use of the relationship
β = p/E
the mass m can be determined.

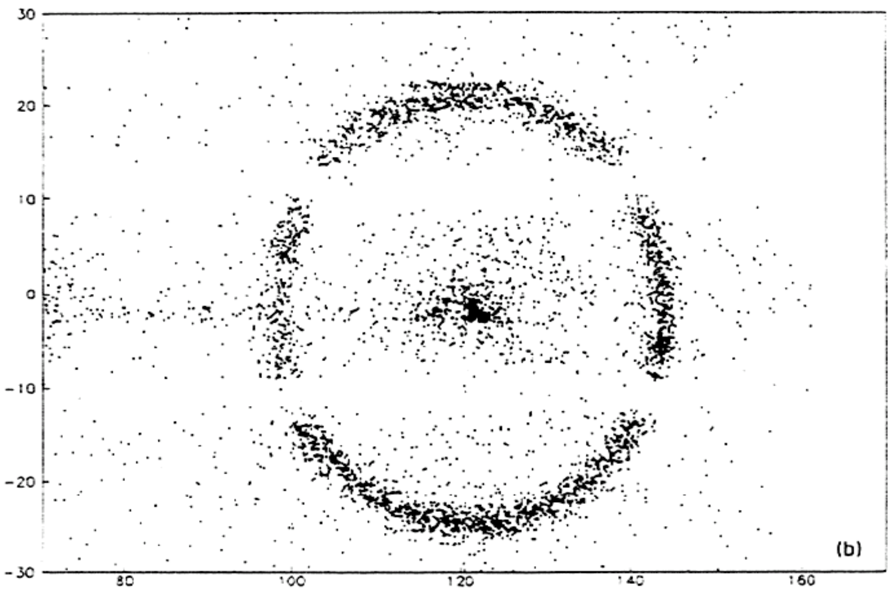

$$\cos\theta = \frac{1}{n\beta} \Rightarrow \theta = \cos^{-1}\left(\frac{\sqrt{m^2+p^2}}{np}\right)$$

For a particle with p=1GeV/c, z = 1, L=1 m, and LiF as the medium (n=1.392) we find:

	θ(deg)	r(m)
π	43.5	0.95
K	36.7	0.75
P	9.95	0.18

Great π/K/p separation!
(until cherenkov angle does not saturate...)

Thus by measuring p and r we can identify what type of particle we have.

Ring Imaging Detectors

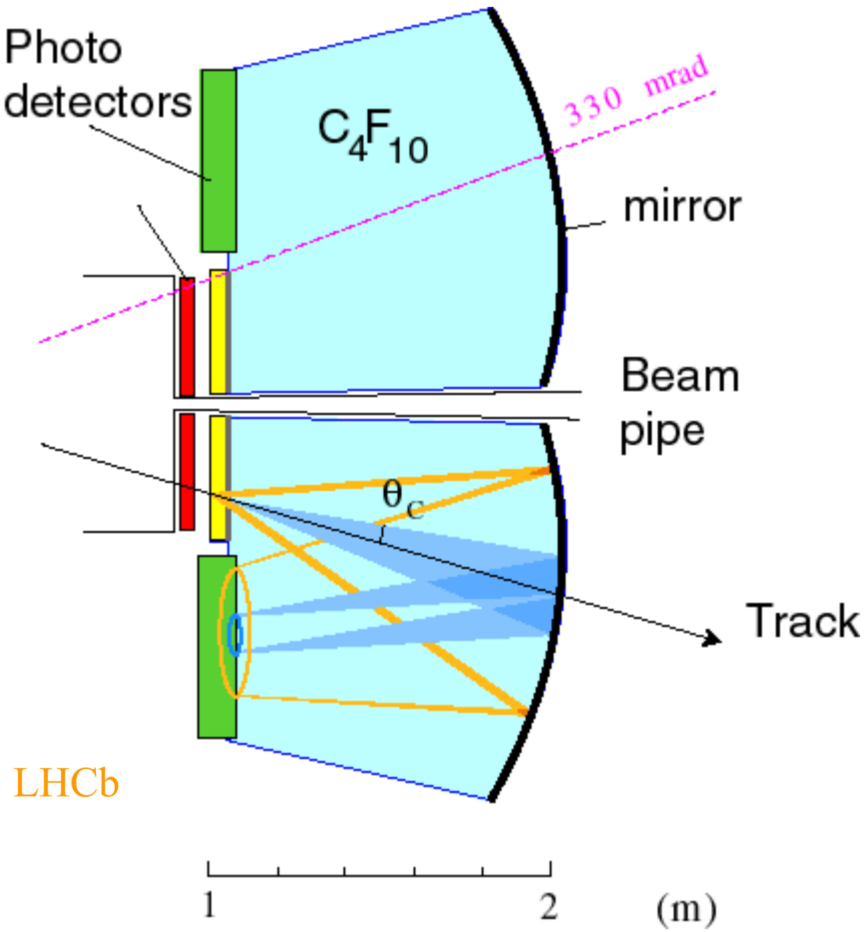

- In accelerator experiments the photodetectors are usually placed as far as possible away from beam.
- Light is reflected by mirrors on the photosensitive detectors
  - Center sets the particle position
  - Radius sets the speed

Ring Imaging Detectors

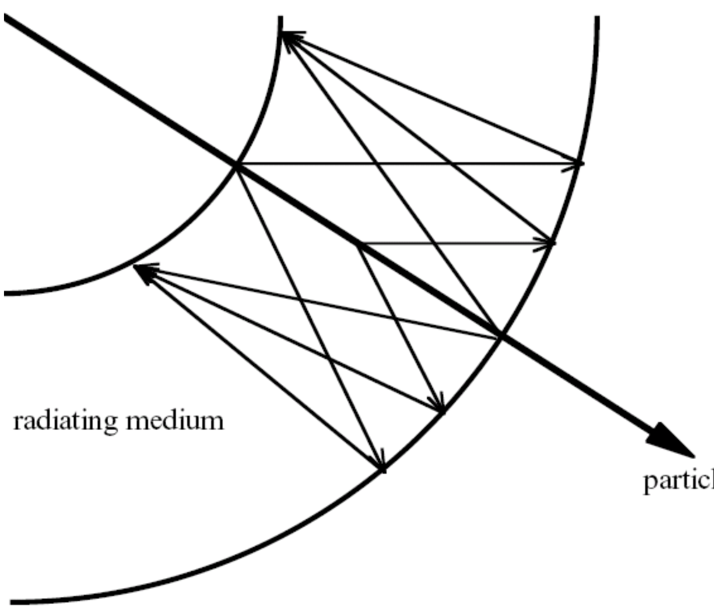

For example a spherical mirror of radius R_S, with centre of curvature coincident with the interaction point (IP), projects the cone of Cherenkov light produced in the radiator onto a ring on the surface of a spherical detector of radius R_D.
The radiator fills the volume between the spherical surfaces with radii R_S and R_D. In general, one takes $R_D = R_S/2$, since the focal length f of a spherical mirror is $R_S/2$.
Because all photons are emitted at same angle θc with respect to the particle trajectory pointing away from the IP, all of them will be focussed to the thin detector ring on the inner sphere. The radius of the Cherenkov ring on the detector surface is

$$r = f \cdot \theta c = R_S \cdot \theta c /2$$

The measurement of r allows one to determine the particle velocity

$$\cos \theta c = 1/n\beta \rightarrow \beta = 1/ n\cos (2r/R_s)$$

Ring Imaging Detectors

The most crucial aspect of RICH counters is the detection of Cherenkov photons with high efficiency on usually large detector surface, since few photons are usually emitted and ever fewer are collected.

Better Cherenkov rings are obtained from fast heavy ions, because the number of produced photons is proportional to the square of the projectile charge.

$$-\frac{dE}{dx} = z^2 \alpha \frac{\hbar}{c} \omega \left(1 - \frac{1}{\beta^2 n^2(\omega)} \right) d\omega$$

The z^2 dependence can be used to measure the absolute charge of incident particle if signal amplitude is measured (ie the # of photons emitted).
This usually done in astroparticle experiments to measure cosmic ray nuclear abundances or in heavy ion collisions

Ring Imaging Detectors

Particle Identification in DELPHI at LEP I and LEP II

→0.7 ≤ p ≤ 45 GeV/c

→15 ≤ θ ≤ 165 mrad

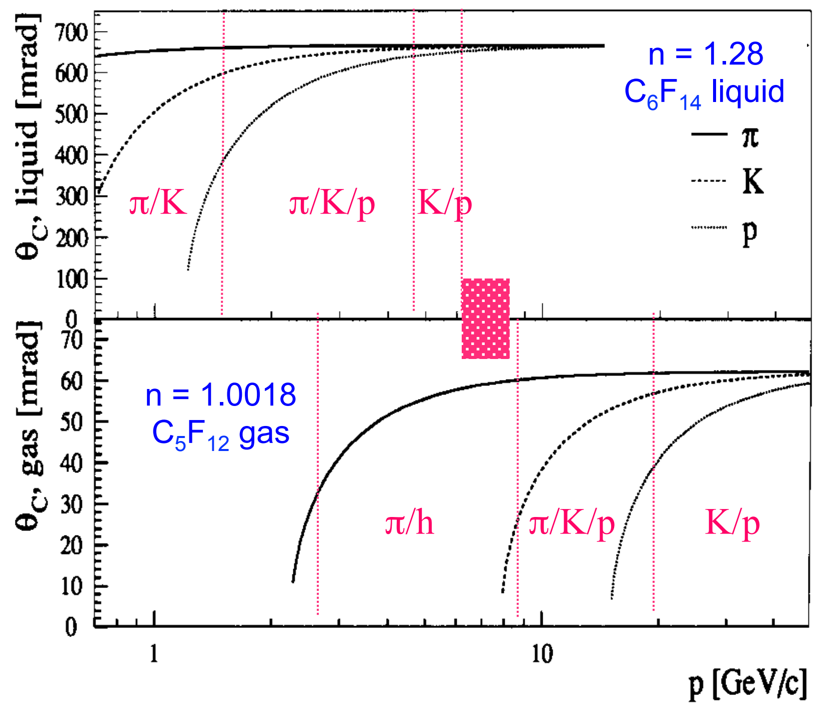

Liquid RICH

Gas RICH

2 radiators + 1 photodetector

Ring Imaging Detectors

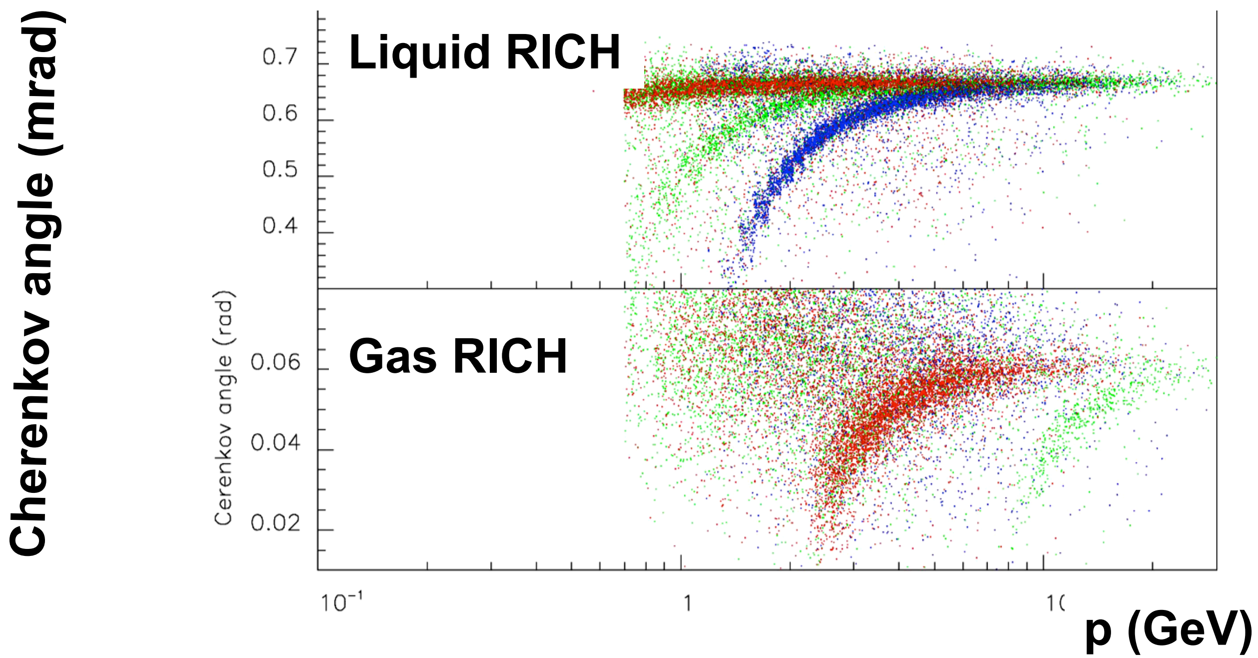

From data

p from Λ K from Φ D* π from K°

Particle ID

- Momentum and speed differ based on the mass of the particle. The nbr. of photons emitted goes as

$$N \approx 1 - \frac{1}{n^2 \beta^2}$$
$$= 1 - \frac{1}{n^2} \cdot \left(1 + m^2 / p^2\right)$$

- Beam magnets can select a fixed momentum.

- Cherenkov counters can identify particles by mass.

5 < p < 12 GeV/c

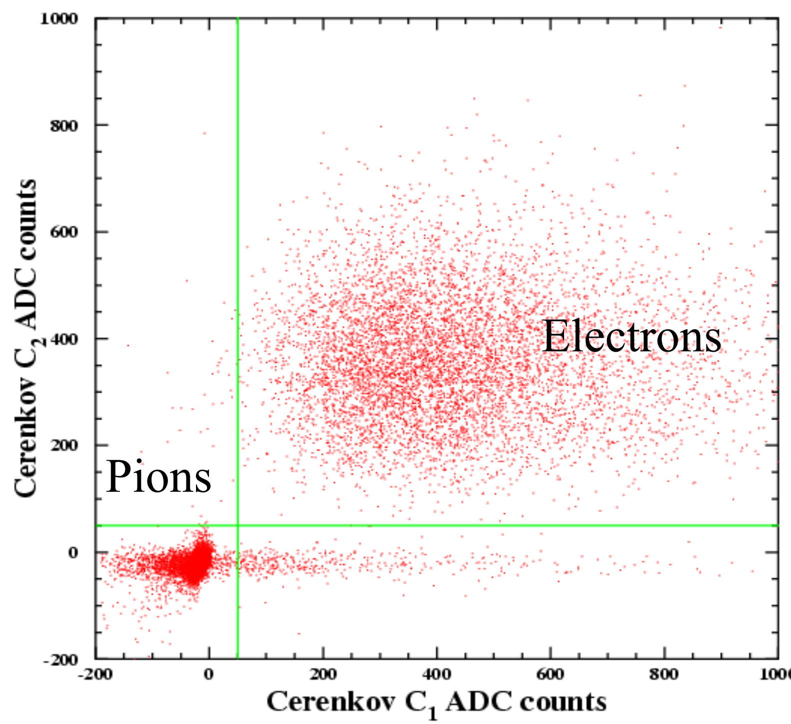

Pions start emission at 17 GeV/c (say, 20 GeV/c)

Mazziotta, GLAST (2005)

NA62 in 1 minuto

Misura di ~100 eventi del decadimento ultra-raro $K^+ \to \pi^+ \nu\nu$

$BR_{exp} = (1.73^{+1.15}_{-1.05}) \cdot 10^{-10}$

$BR_{th} = (0.78 \pm 0.08) \cdot 10^{-10}$

Estrema precisione, estrema sensibilità a NP

Nuova tecnica: decadimento in volo ad alta energia

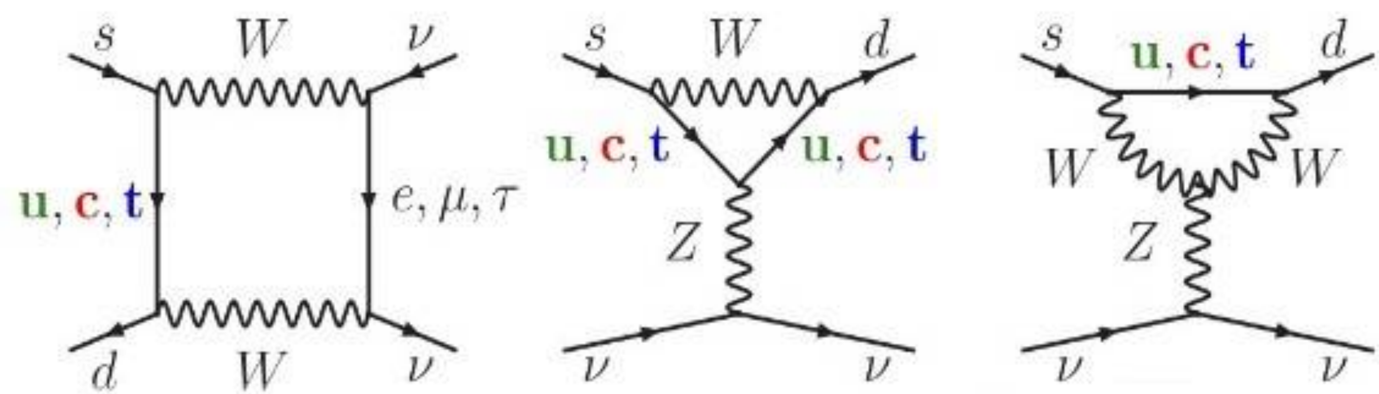

Schema del rivelatore

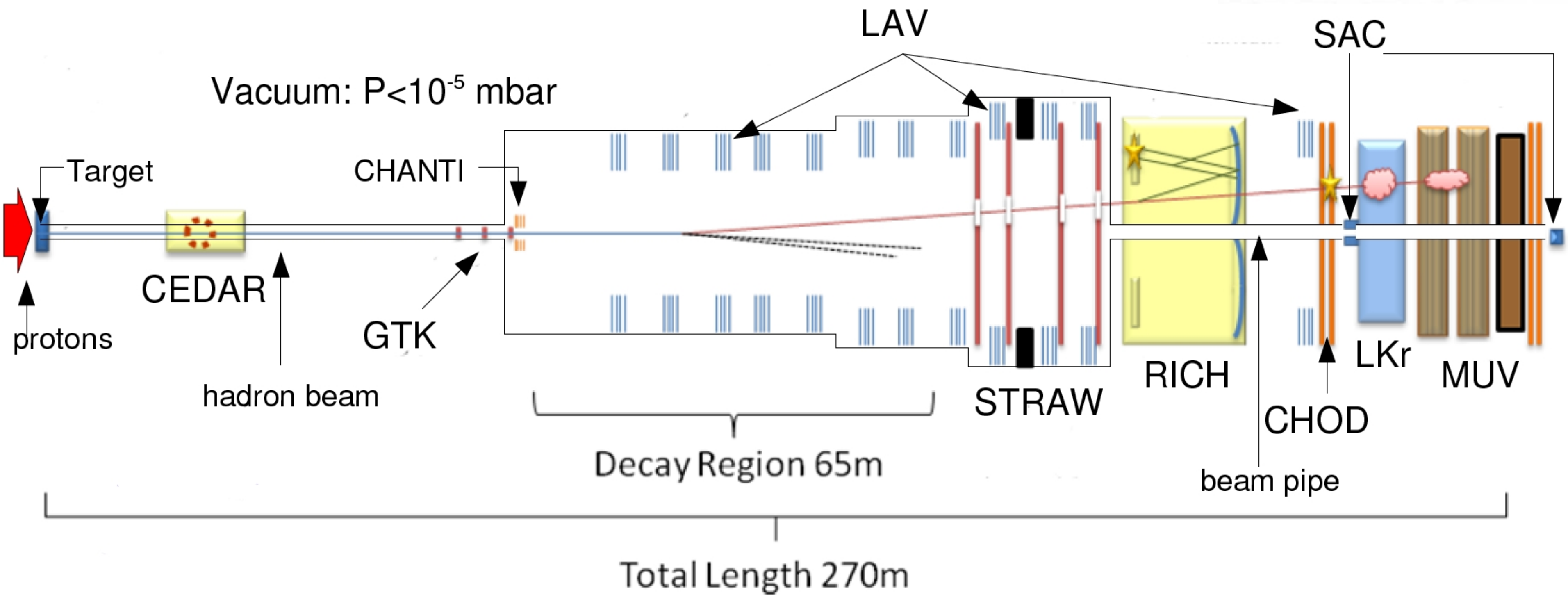

- Decadimenti di Kaoni in volo da un fascio “non separato” a 75 GeV/c, prodotto da un fascio di protoni a 400 GeV/c estratto dall’SPS contro un bersaglio fisso di berillio (fascio a ~800 MHz, ~6% kaons)
- Le particelle non decadute viaggiano nel tubo a vuoto centrale
- Goal: misura di O(100) eventi in 2 anni di presa dati riducendo l’errore sistematico fino al livello di qualche %

Background suppression

Signal: $BR_{TH}(K^+ \to \pi^+ \nu\nu) = (0.85 \pm 0.07) \times 10^{-10}$ SM@NLO

Impossibile visualizzare l'immagine. La memoria del computer potrebbe essere insufficiente per aprire l'immagine oppure l'immagine potrebbe essere danneggiata. Riavviare il computer e aprire di nuovo il file. Se viene visualizzata di nuovo la x rossa, potrebbe essere necessario eliminare l'immagine e inserirla di nuovo.

- Main background:
  $K^+ \to \mu^+\nu$ ($K_{\mu 2}$) BR = 63.4%
- Rejection factor at least 10^{-12}
  - Kinematics : $\sim 10^{-5}$ → Straw tracker + GTK
  - Veto for muons $\sim 10^{-5}$ → Muon Veto
  - Particle Identification:

    μ suppression < 5×10^{-3}

RICH

- Precise K-π timing
  time resolution: $\leq$ 100 ps

Decay	BR
$\mu^+\nu$ ($K_{\mu 2}$)	63.5%
$\pi^+\pi^0$ ($K_{\pi 2}$)	20.7%
$\pi^+\pi^+\pi^-$	5.6%
$\pi^0 e^+\nu$ (K_{e3})	5.1%
$\pi^0\mu^+\nu$ ($K_{\mu 3}$)	3.3%

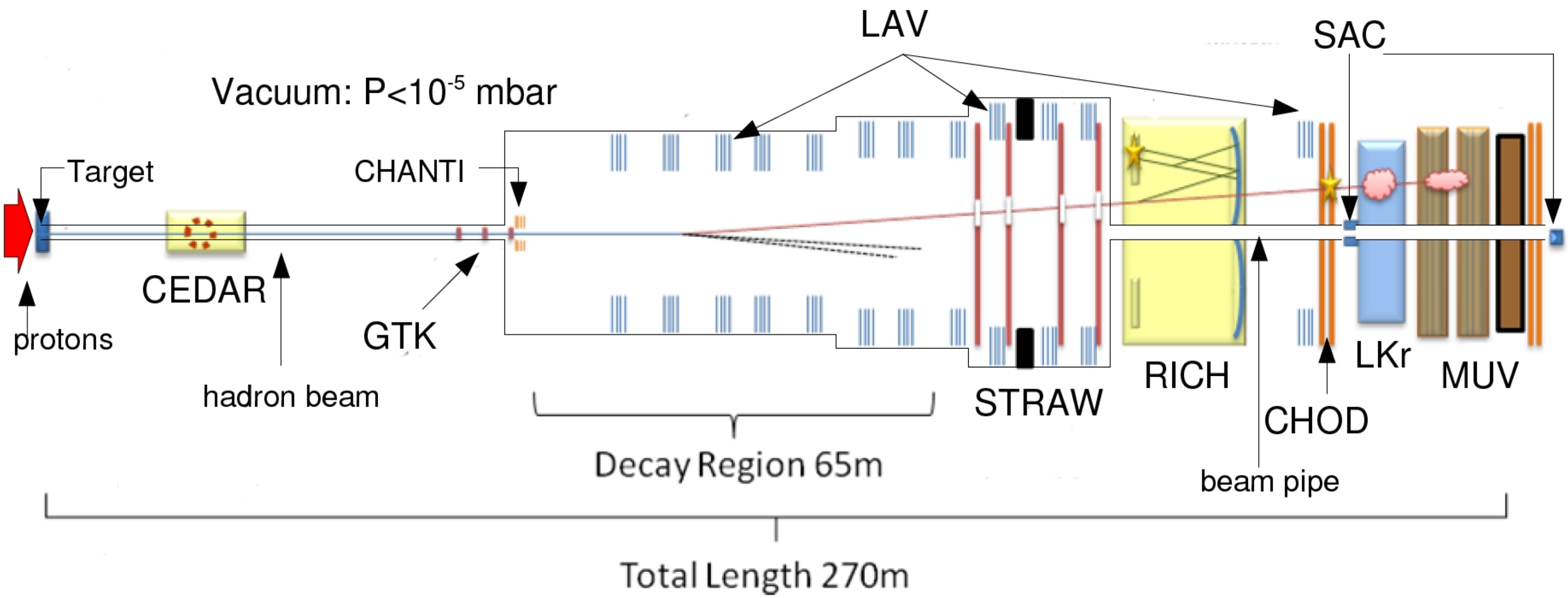

The kaons are produced by protons from the CERN SPS hitting a fixed target. Down-stream of the target, an achromatic system selects charged particles with 75 GeV/c momentum. These particles (of those about 6% are kaons) are tagged and measured by a silicon pixel detector, working at a rate of 1 GHz (GigaTracker). The kaons decay then in flight in a 80 m long vacuum vessel. The pion track is measured in a spectrometer, made from 4 straw chambers, two before and two after a dipole magnet. To reduce multiple scattering, the straw tubes are operated in vacuum. Background arises from mainly two decay channels: $K^+ \rightarrow \pi^+ \pi^0$ and $K^+ \rightarrow \mu^+ \nu$, which together are responsible for about 87% of all kaon decays. For suppression of the $\pi^+ \pi^0$ decay, several sets of photon veto-counters reject all events with additional photons. A large angle veto (LAV), made from several rings of lead glass scintillator around the vacuum vessel, detects photons which leave the detector on the outside. The main photon rejection is performed by a liquid-krypton calorimeter (LKr), already used in the NA48 experiment, with excellent energy resolution and granularity. Finally, calorimeters at the end of the beam pipe detect photons which are emitted along the beam line. The rejection of $K^+ \rightarrow \mu^+ \nu$ decays is partly done kinematically by the momentum measurement in the straw chambers. However, to achieve the required rejection power of about 10^{11}, we need a good muon-pion identificatio in addition. This is performed by a RICH detector, the LKr calorimeter and a new muon veto detector, which measures the shower shape of pion and muon showers in matter.

PID dei K del fascio

Scopo: Identificazione del Kaone nel fascio non separato per associarlo temporalmente ai prodotti di decadimento rivelati a valle. Questo permette di rilasciare le condizioni sullo scattering multiplo nel gas residuo presente nella zona di decadimento (è sufficiente ottenere un vuoto a livello di 10^{-5} mbar).

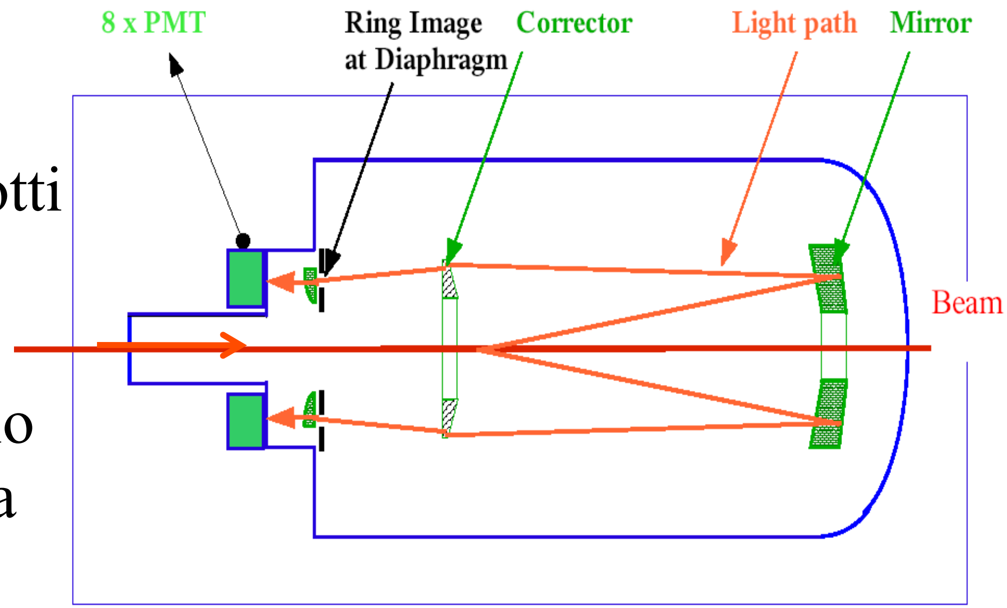

Tecnica: Rivelatore Cherenkov differenziale (il radiatore e H_2)

- Riutilizzabile un vecchio rivelatore costruito al CERN negli anni '70
- Nuovo readout (fotomoltiplicatori e elettronica di lettura)
- Nuovo sistema di specchi deflettori per diminuire il rate sul singolo canale in lettura

Il RICH di NA62

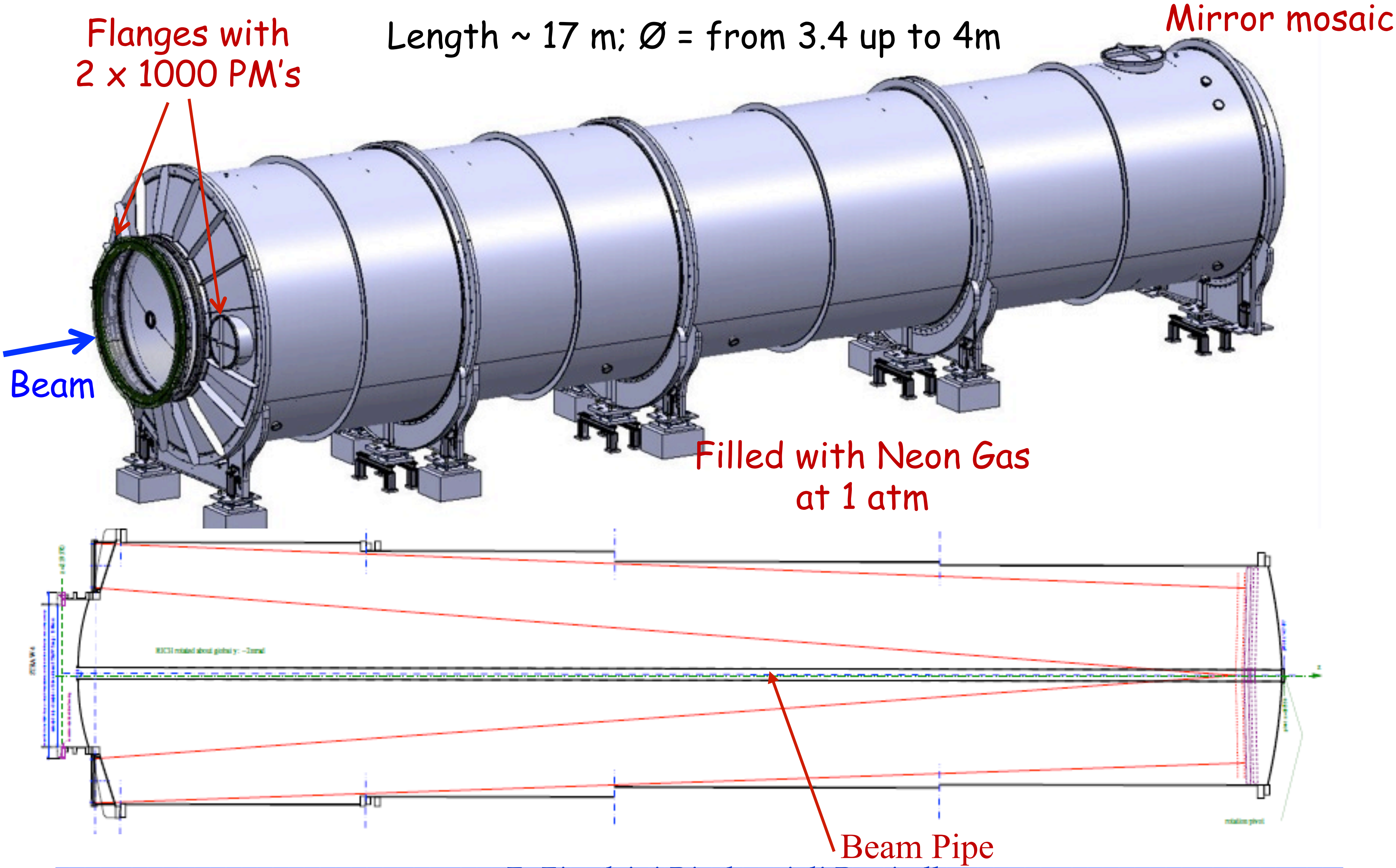

The NA62 RICH

3σ $\pi - \mu$ separation (15-35 GeV/c)

- Neon at 1 atm (π thresh.:12 GeV/c)
- 2000 PMT
- 18 mm pixel
- 100 ps

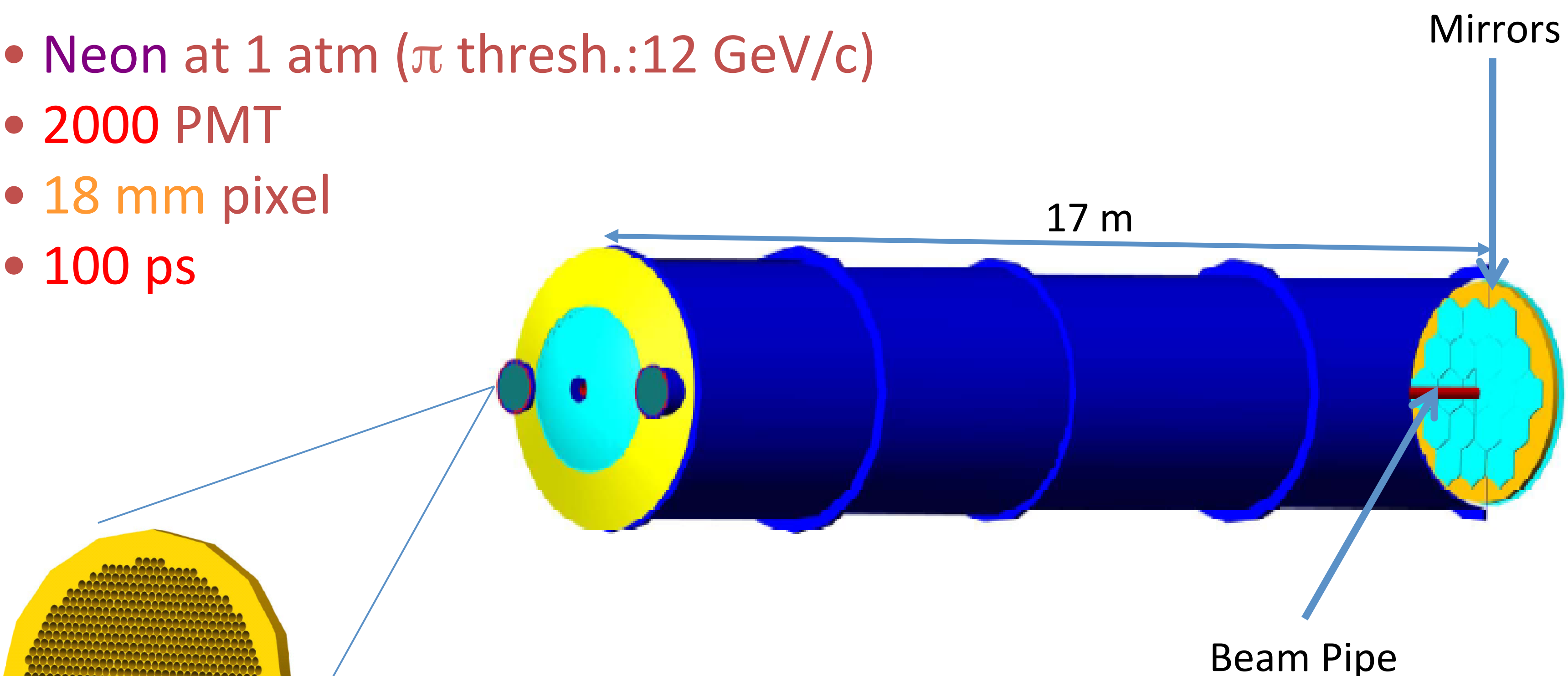

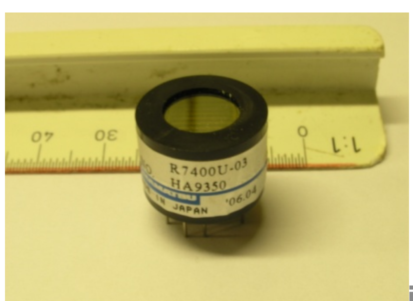

PMT: Hamamatsu R7400 U03

The NA62 RICH tasks

- Separate π-μ in $15 < p < 35$ GeV/c with a muon suppression factor better than 5×10^{-3}
- Measure pion crossing time with a resolution < 100 ps
- Provide a L0 trigger for charged tracks

Radiator: Neon gas at atmospheric pressure

- full efficiency requires → $p_{threshold} = m / \sqrt{(n^2-1)} = 12.5$ GeV/c for π
- $(n-1) = 62.8\ 10^{-6}$ at λ=300 nm (small dispersion)
- appropriate refractive index at atmospheric pressure (non-flammable)
- good light transparency in visible and near-UV, low chromatic dispersion
- low atomic number → small X_0
- $\theta_{C\ max} = 11.2$ mrad

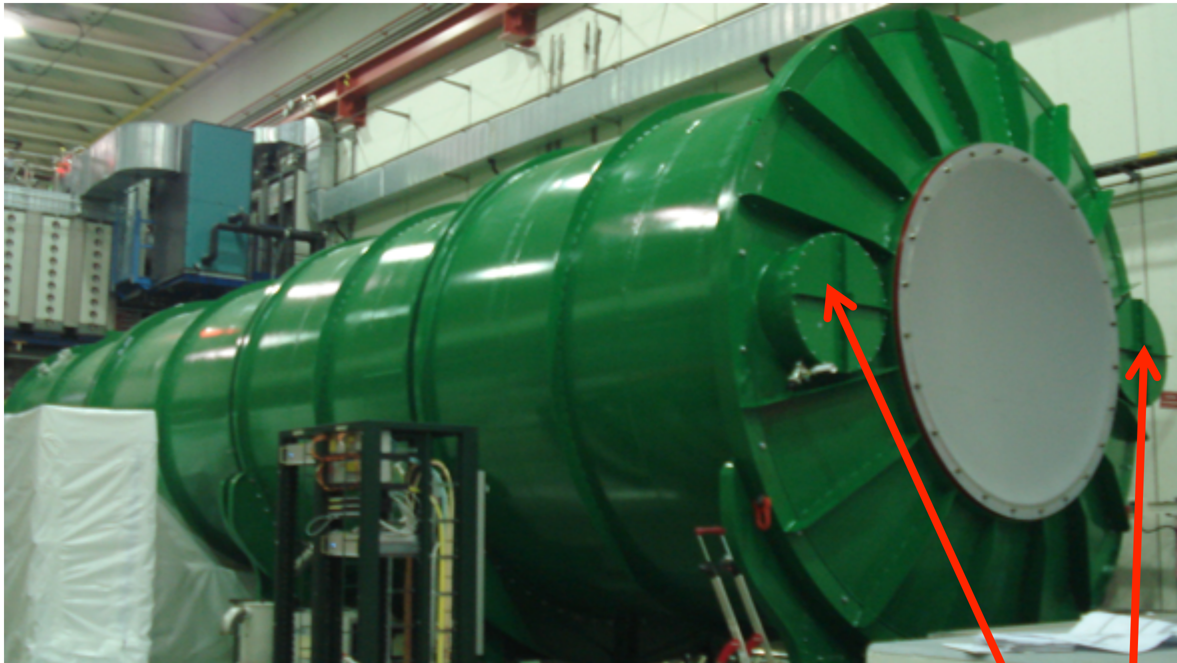

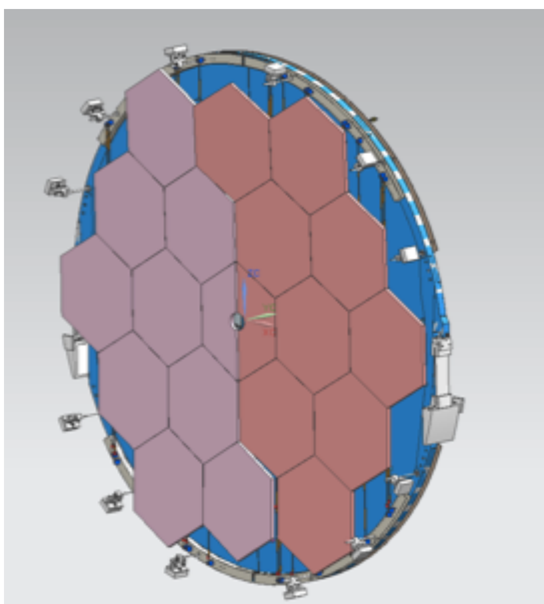

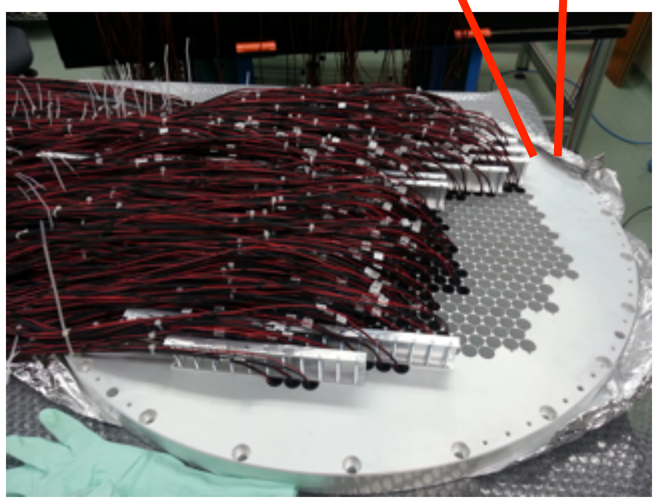

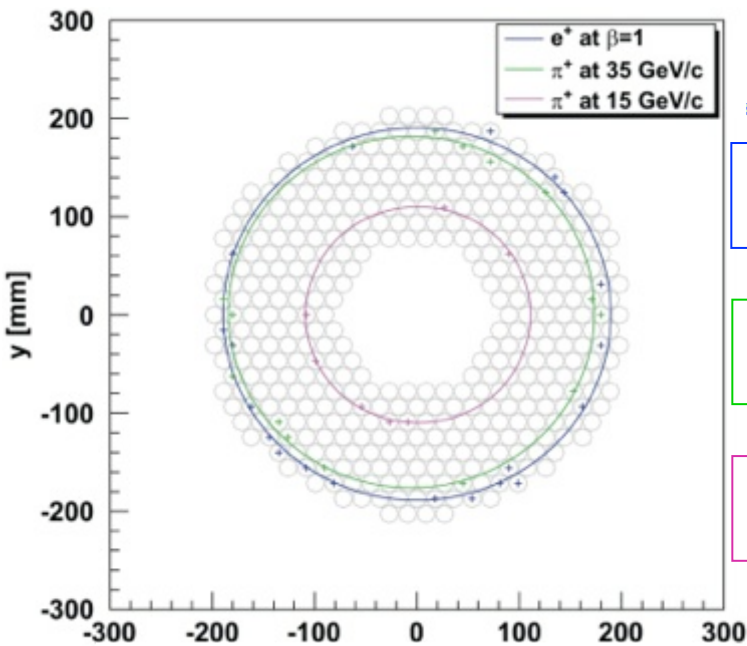

Typical data events with fitted rings

positrons at β=1

pions at 35 GeV/c

pions at 15 GeV/c

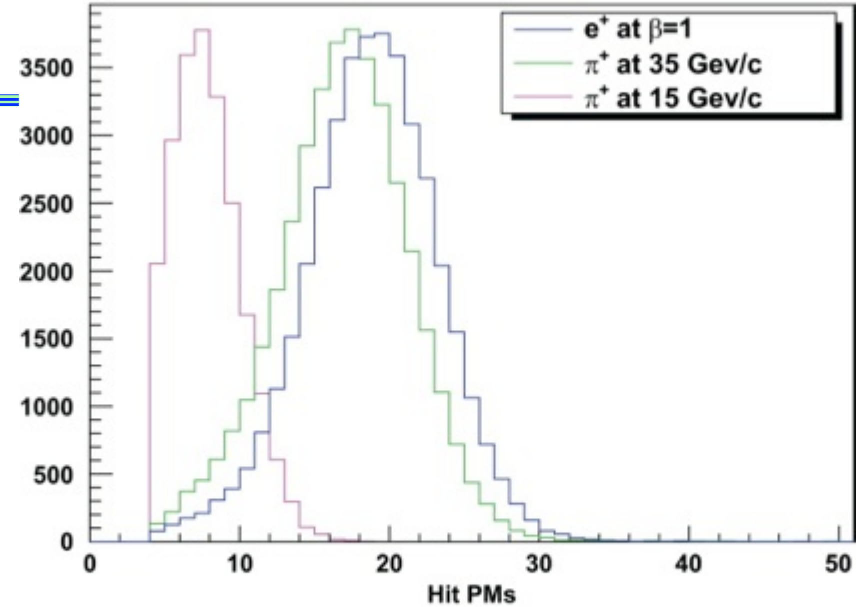

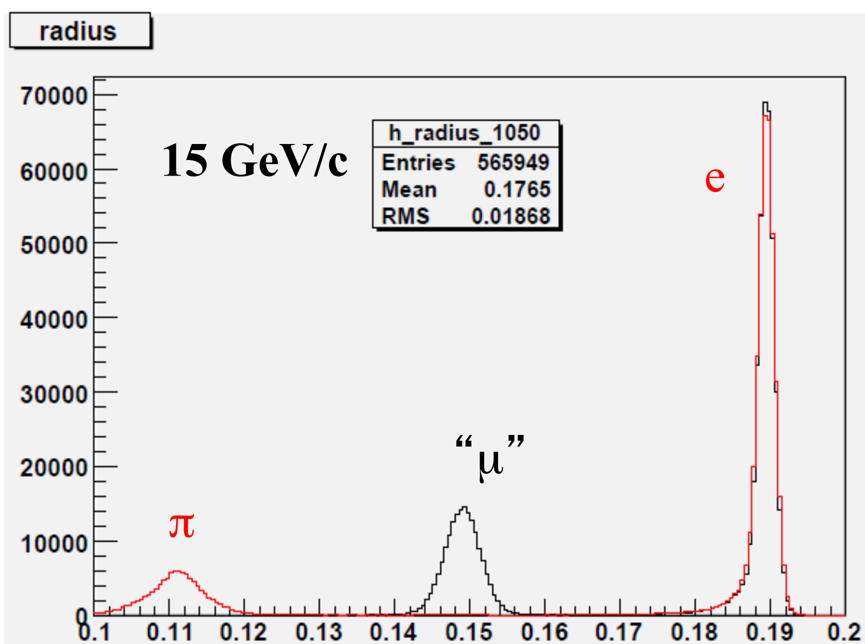

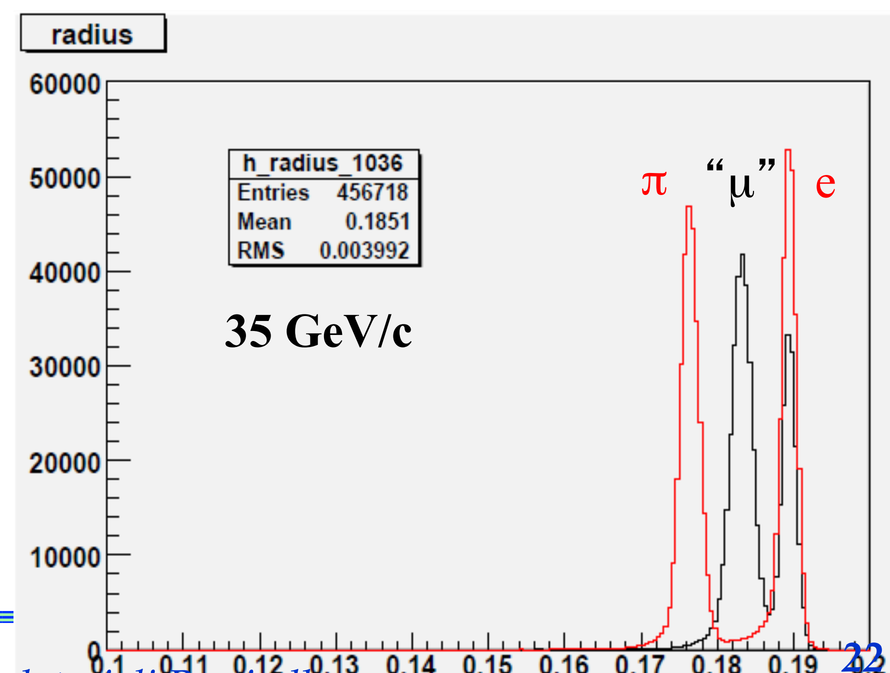

RICH-400: fitted rings

20 GeV/c

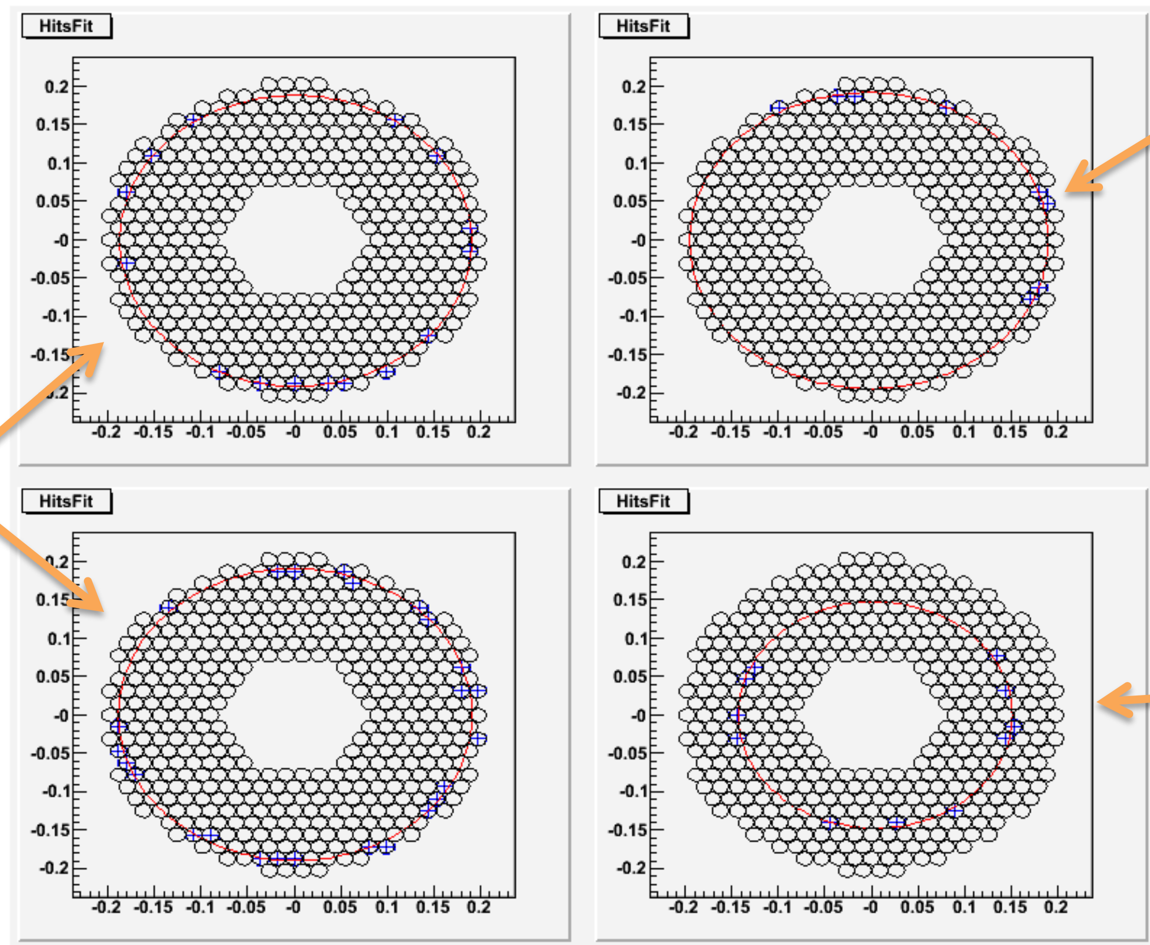

Hard to reconstruct ring…

positrons

pion

Few photons, no complete rings, difficult to fit, ie bigger uncertainties

AMS-02

TRD (|Q|, e/p)

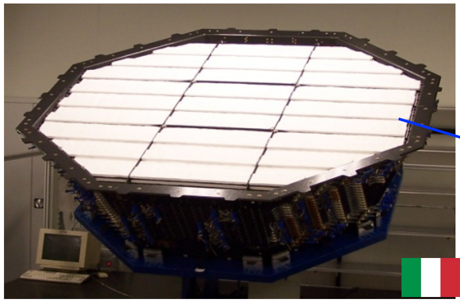

Silicon Tracker (±Q,E)

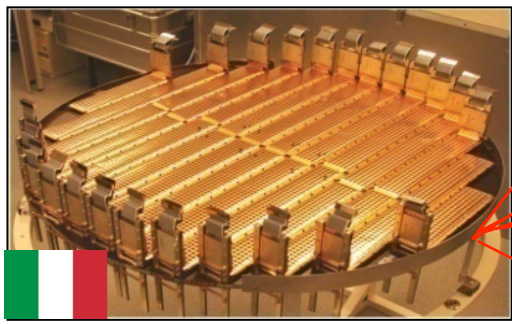

ECAL (E, e/p)

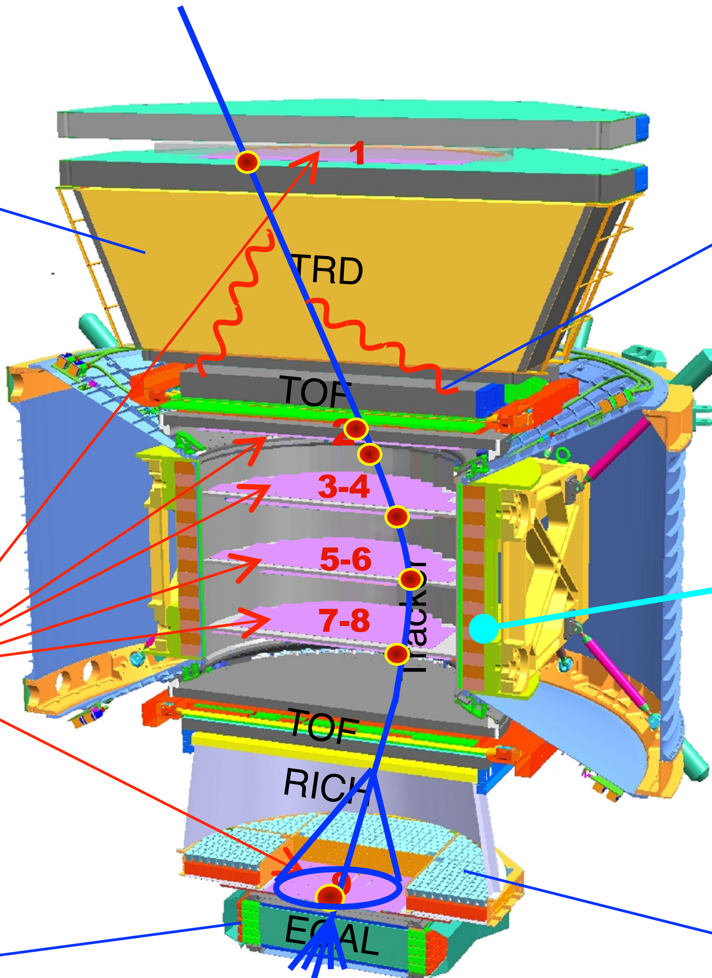

TOF (v, |Q|, trigger)

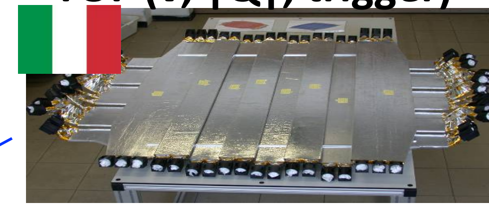

Permanent Magnet

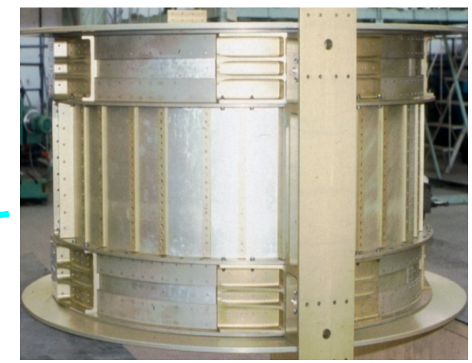

RICH (v,|Q|)

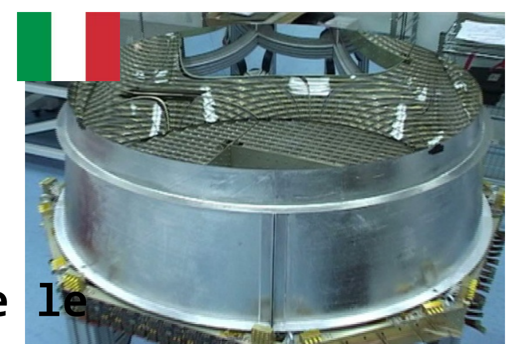

Occorre misurare Q, E, v
Note v ed E, si ricava m
Misure multiple per minimizzare le
incertezze sperimentali

AMS Ring Imaging Cerenkov Counter

- Accurate Velocity Measurements → Isotopic Separation.
- |Q| measurements
- $\Delta\beta/\beta \sim 0.1\%$
- Additional Particle Identification capability

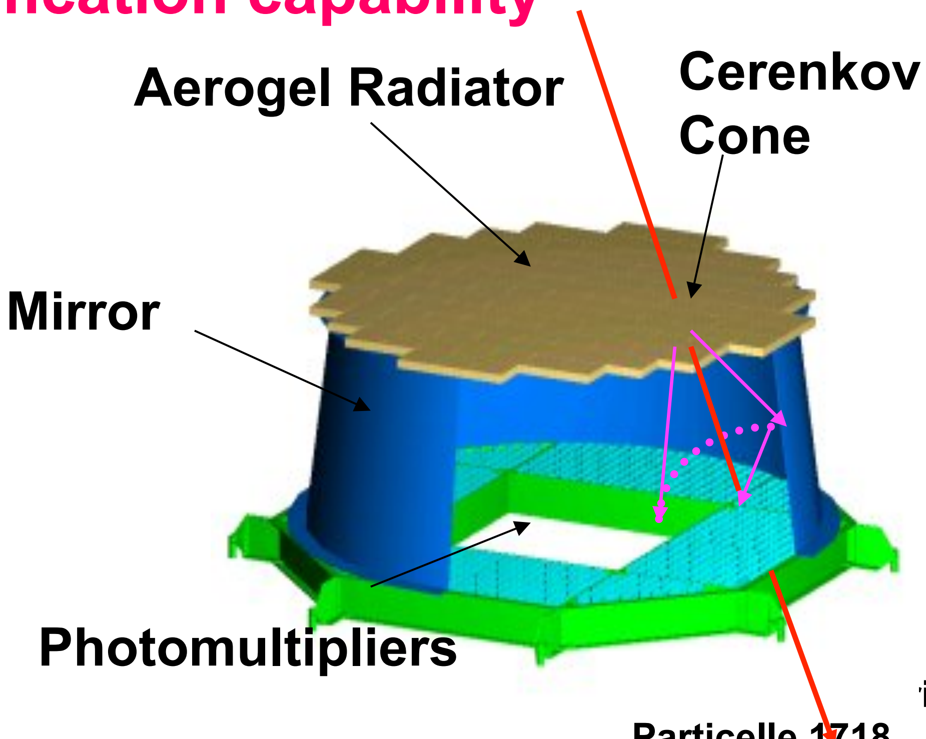

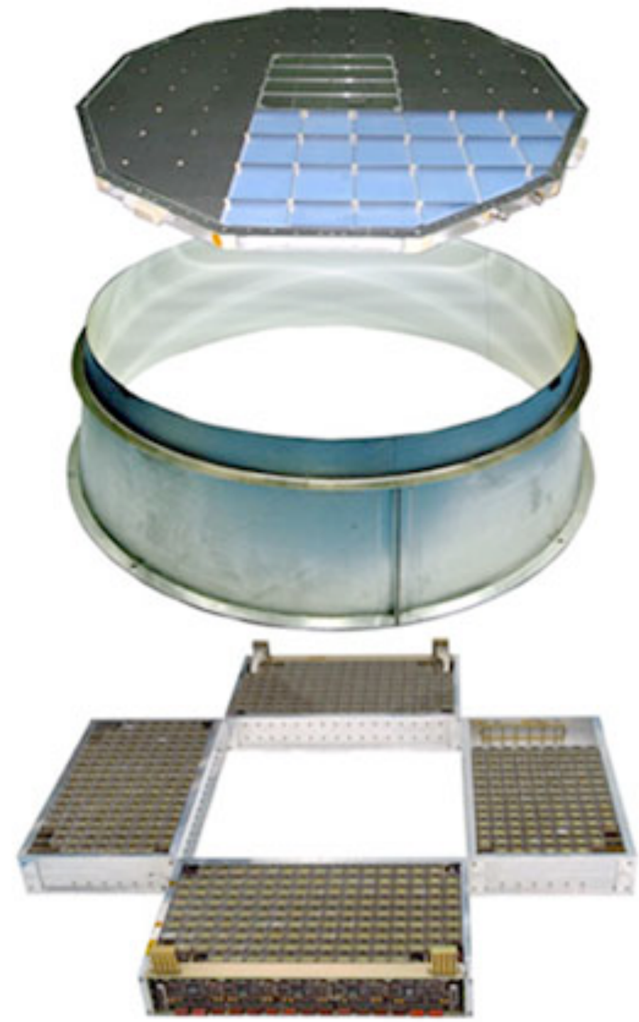

Operation Principle

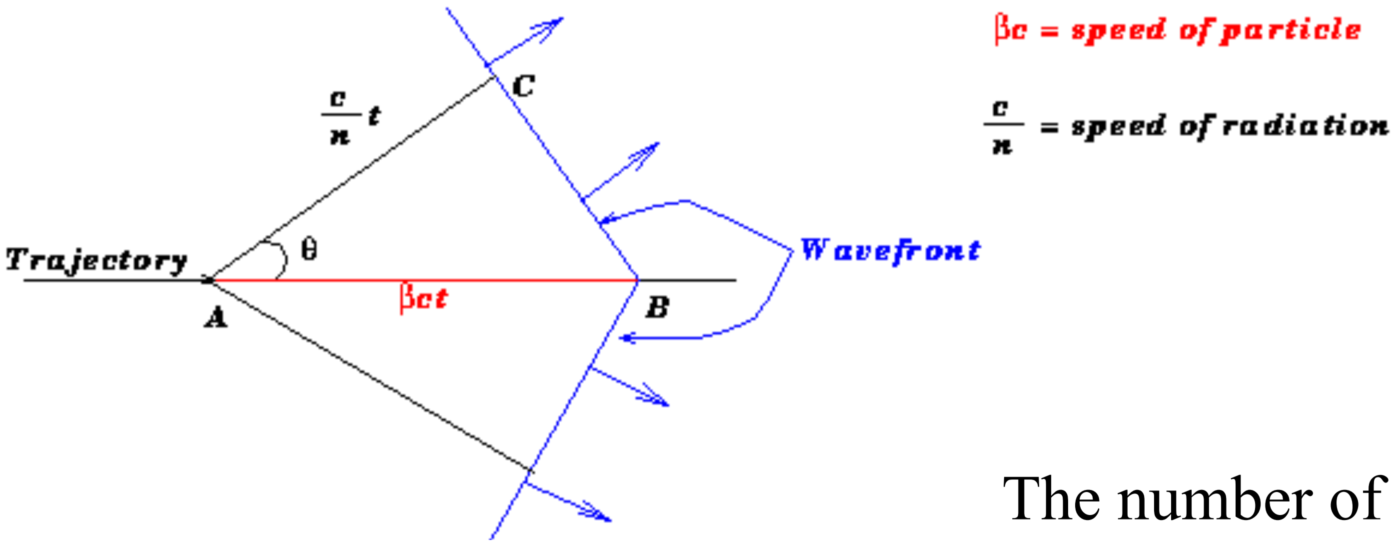

The number of emitted photons is ∝ L $Z^2 \langle \sin^2\theta_c \rangle$

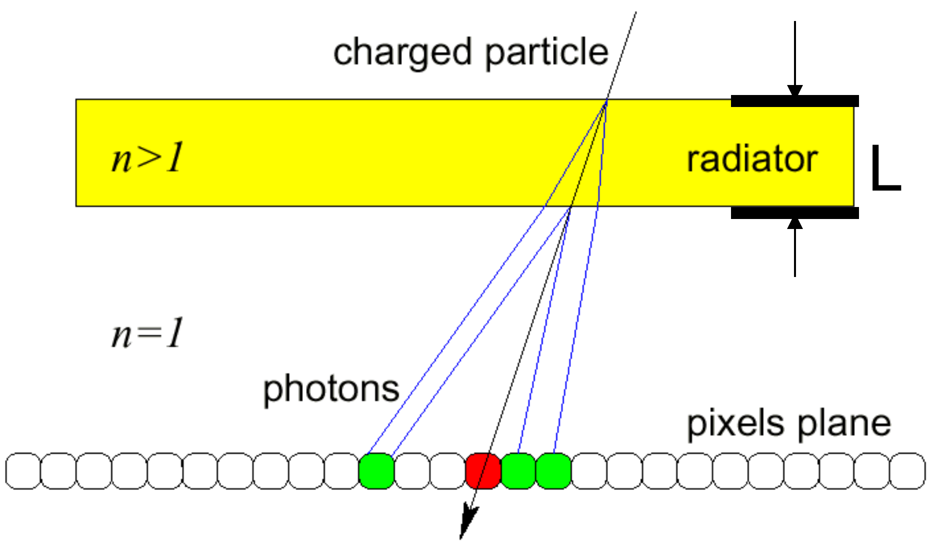

These can be detected with a ph sensitive detector, e.g. PMT

RICH

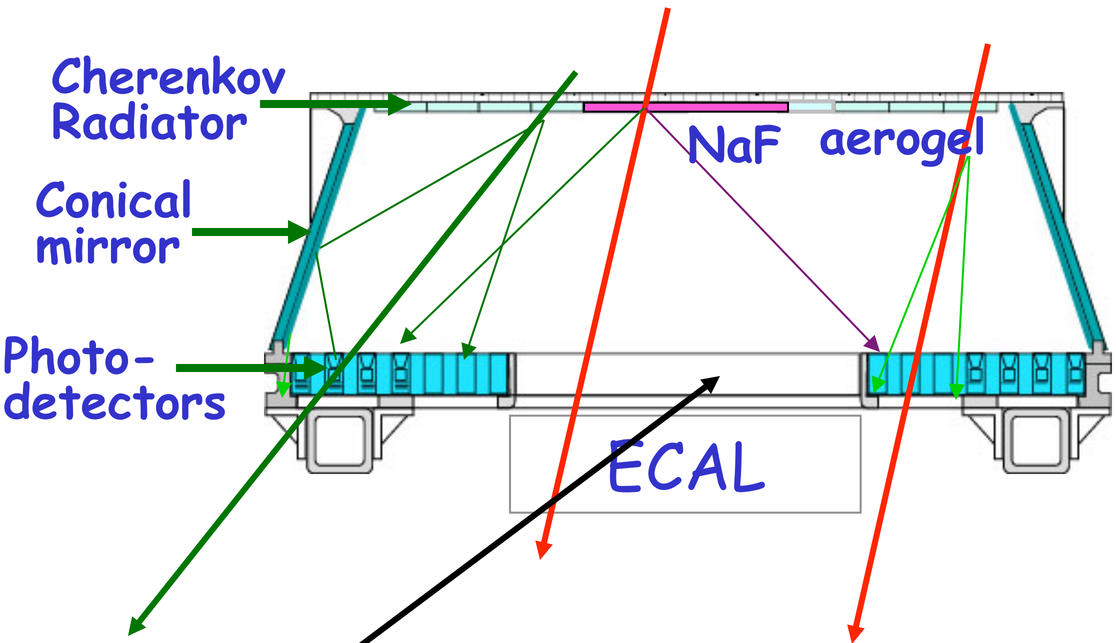

RICH is made by a radiator plane and a photodetector plane. The conical mirror increases the acceptance for particles incident at large angles for which the Cerenkov photons would miss the detection plane

Because of the ECAL below RICH, the central part of the detector cannot be filled with to avoid material in front of the ECAL

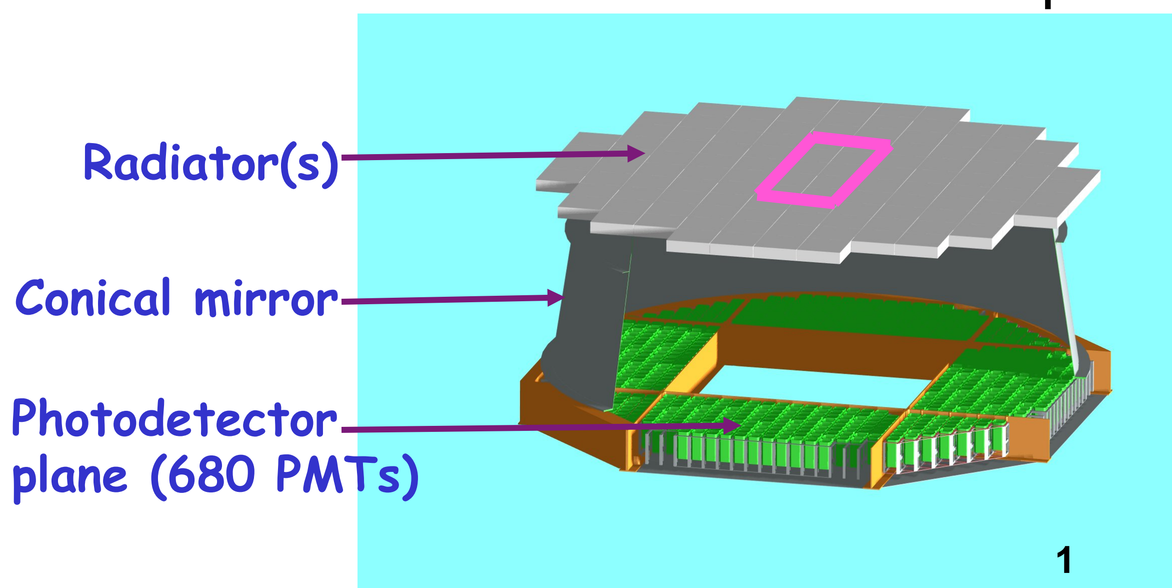

Radiator plane

The radiator plane is made of two different materials:

- the central part, above the ECAL hole, is a 5 mm layer of sodium fluoride NaF with large refractive index, n=1.33
- the outer part is a 30 mm layer of aerogel with refractive index close to 1, n=1.03-1.05

Particles hitting the NaF, will emit radiation at large angles because of n_{NaF} → it will miss the hole (e.g. for $\beta=1$, $\theta_c=41^o$ and $r=L\,tg\theta_c=42$ cm)

When hit the aerogel, θ_c (14^0 @ $\beta=1$) is small and again the radiation will not enter the hole

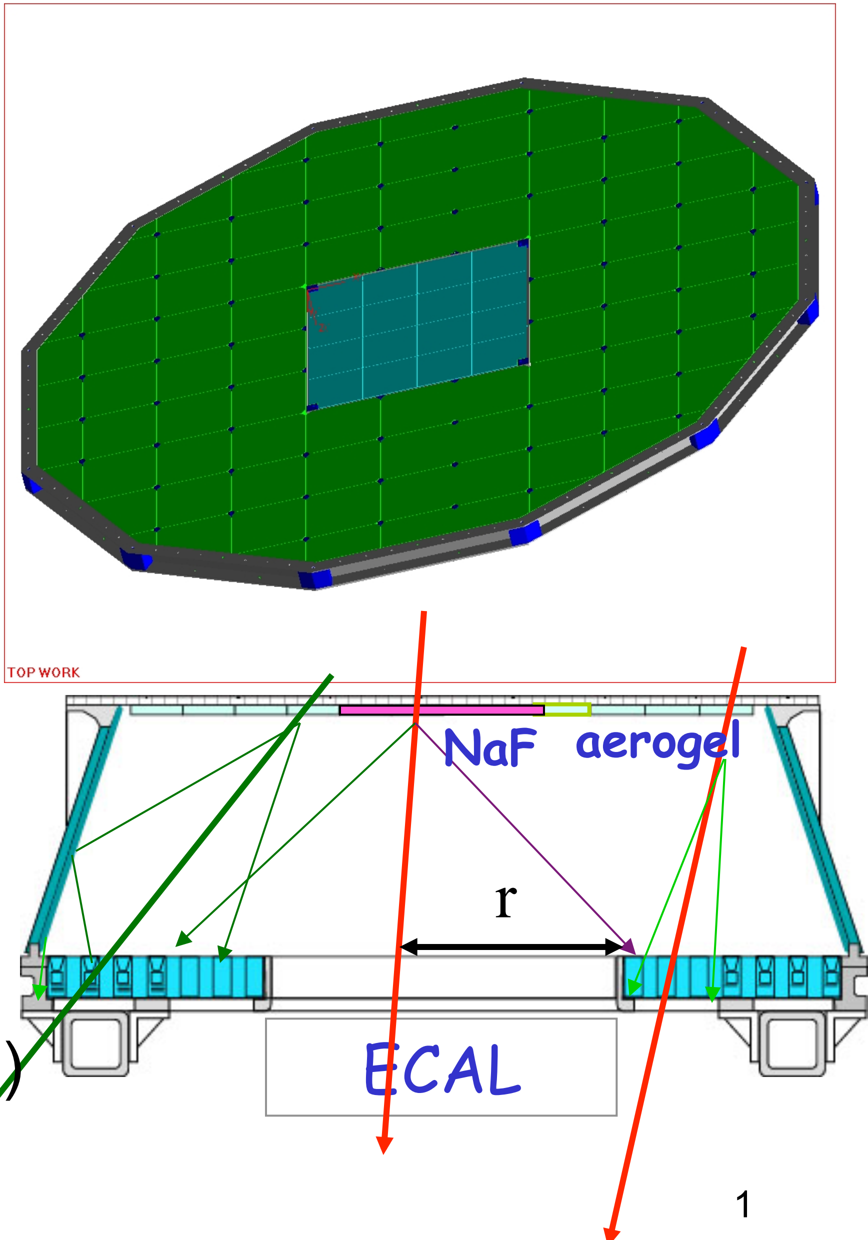

RICH images

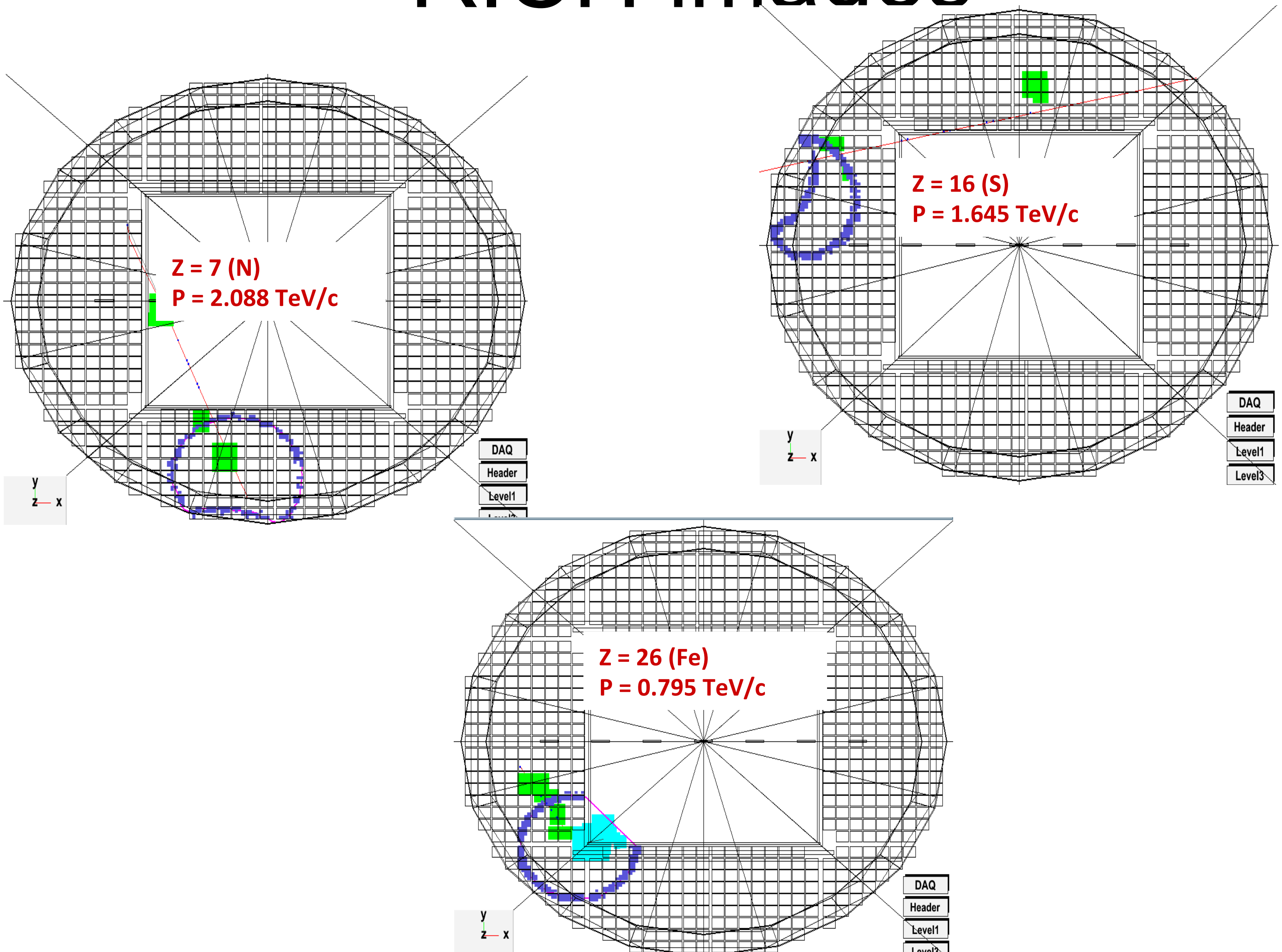

Z = 7 (N)
P = 2.088 TeV/c
Z = 16 (S)
P = 1.645 TeV/c
Z = 26 (Fe)
P = 0.795 TeV/c
DAQ
Header
Level1
Level3

Rich performances

From "rings" radius it is possible to measure β
From the signal intensity it is possible to measure $|Z|$
If the particle does not arrive perpendicular to the radiator plane, the cone projection on the photon detector plane is not a circle, so it is needed to know the particle direction (with an other detector).

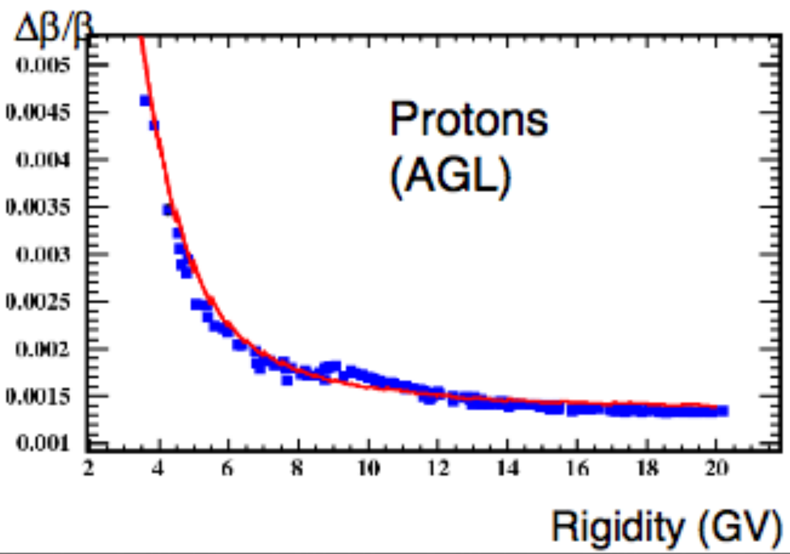

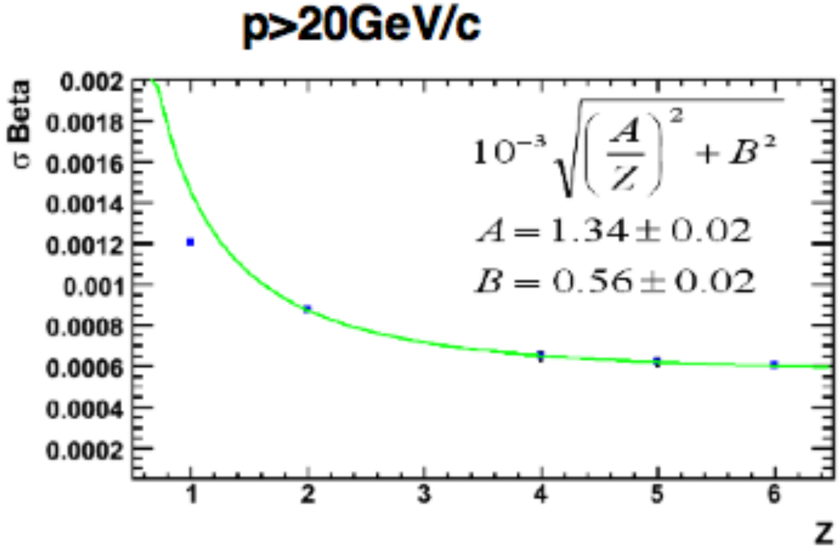

RICH Z measurement *(F. Barão & R. Pereira work)*

Z uncertainties:

- ✓ statistical
- ✓ systematics from non-uniformities:
  - ✓ radiator: n, thickness, clarity, ... (data base with values)
  - ✓ detection: LG, PMT, temperature effects

$$\boxed{\Delta Z = \frac{1}{2}\sqrt{\frac{1+\sigma^2_{p.e}}{N_0} + Z^2\left(\frac{\Delta\varepsilon}{\varepsilon}\right)^2}}$$

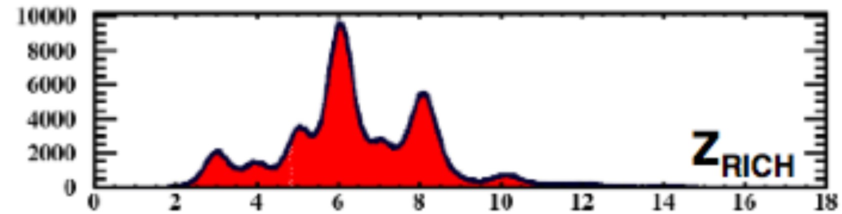

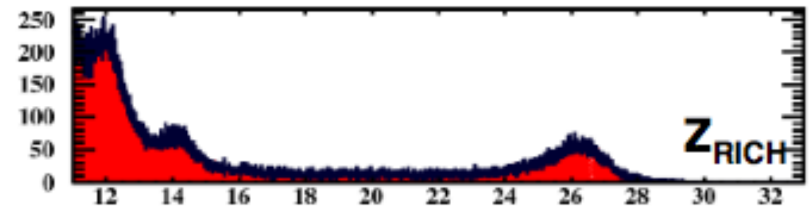

Charge corrections apllied:

- ✓ PMT gain
- ✓ Cell efficiency (light transmission in LG, PMT/pixel quantum eff) **Time independent**
- ✓ Temperature effects (gains and eff) **Time dependent**

	uncorr	time-ind corr	+time-dep corr	final
σ stat	0.295	0.288	0.283	**0.283**
σ syst	5.20%	3.45%	2.77%	**2.56%**

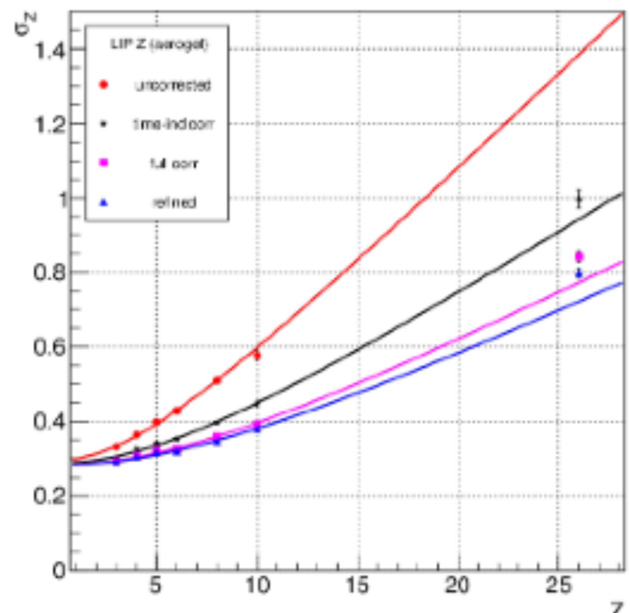

Neutrino ID

Another example of particle identification by Cherenkov rings comes from neutrino physics.

An important aspect of atmospheric neutrino studies is the correct identification of neutrino-induced muons and electrons.

Figures 9.13 and 9.14 show a neutrino-induced event ($\nu\mu + N \rightarrow \mu- + X$)

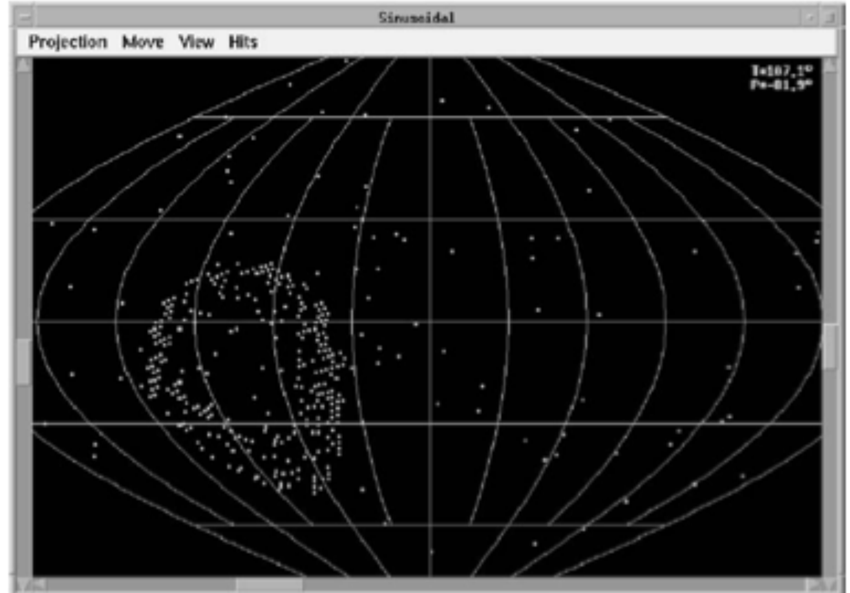

Muons from μ-neutrinos make a clean ring.

Fig. 9.13. Neutrino-induced muon in the SNO experiment [53].

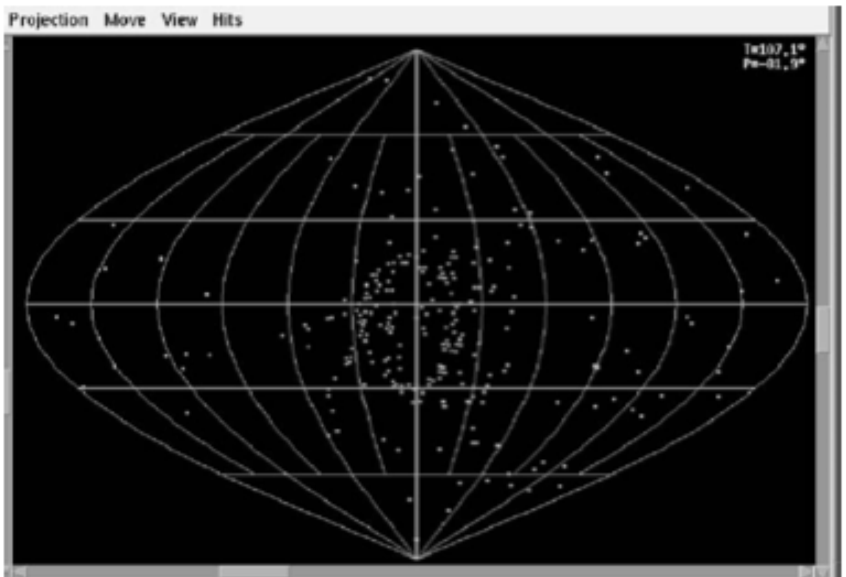

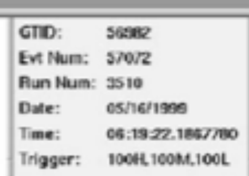

e from *e*-neutrinos make a diffuse ring.

e- interact and shower

Fig. 9.14. Cherenkov ring produced by an electron from muon decay, where the muon was created by a muon neutrino [53].

with subsequent (0.9 μs later) decay $\mu- \rightarrow e- + \bar{\nu}e + \nu\mu$ in the SNO experiment which contains a spherical vessel with 1000 tons of heavy water viewed by 10 000 PMTs. The particle-identification capability of large volume neutrino detectors is clearly seen.

Neutrino ID

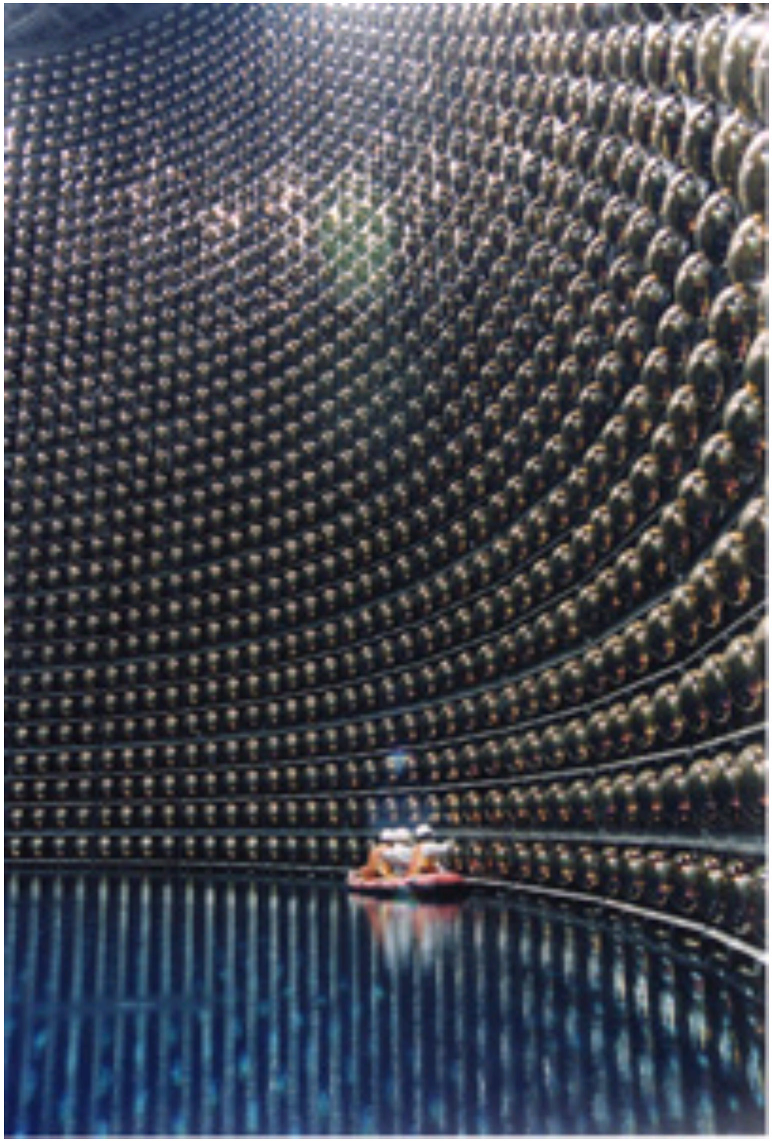

Super Kamiokande

- Cherenkov imaging is used in neutrino detectors.
  - Underground observatories

Radiazione di transizione

C'e' un altro fenomeno di emissione importante per la rivelazione delle particelle, che non e' dovuto all'accelerazione della particella ma alla sua interazione con il mezzo: la radiazione di transizione

Transition radiation

- **Transition radiation** is the radiation from a uniformly moving charge in a medium with a variable dielectric constant. Typically, it is produced by relativistic charged particles when they cross the interface of two media of different dielectric constants
- It is analogous to the radiation from a particle moving non-uniformly. In both cases the radiation is related to the phase velocity of the electromagnetic waves in the given medium and the velocity of the charged particle.
- The emission depends on the time variation of $\beta = nv/c$ (n=refractive index)
- The difference is that in the former case the phase velocity of the wave changes, while in the latter particle velocity changes. (In this sense, TR and bremsstrahlung have the same origin.)
- The emitted radiation is the homogeneous difference between the two inhomogeneous solutions of Maxwell's equations of the electric and magnetic fields of the moving particle in each medium separately. In other words, since the electric field of the particle is different in each medium, the particle has to "shake off" the difference when it crosses the boundary.

Radiazione di transizione

La radiazione di transizione è emessa quando una particella carica attraversa la superficie di discontinuita' tra due mezzi con indici di rifrazione diversi, e.g. alla superfice di separazione fra il vuoto e un dielettrico.

L'emissione e' legata alla polarizzazione del mezzo indotta dai campi della particella incidente: i campi variabili della particella incidente inducono una polarizzazione P(**x**,t) dipendente dal tempo.

La polarizzazione emette radiazione.

I campi irraggiati si sommano coerentemente vicino alla traiettoria della particella e per un certo spessore nel mezzo, dando luogo ad una radiazione di transizione con una distribuzione angolare e un'intensita' caratteristiche

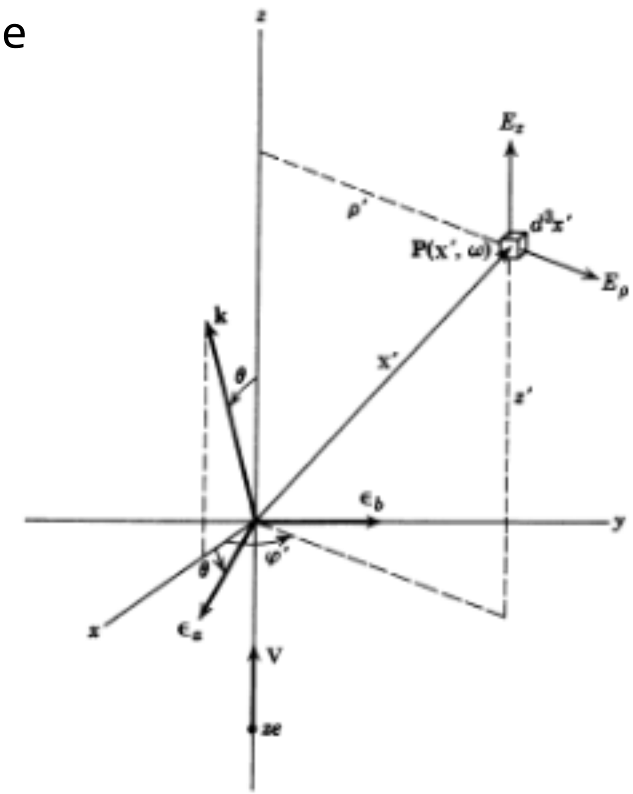

Figure 13.9 A charged particle of charge ze and velocity **v** is normally incident along the z axis on a uniform semi-infinite dielectric medium occupying the half-space $z > 0$. The transition radiation is observed at angle θ with respect to the direction of motion of the particle, as specified by the wave vector **k** and associated polarization vectors ϵ_a and ϵ_b.

Radiazione di transizione

Per gli immancabili entusiasti dei calcoli, una trattazione della radiazione di transizione si trova in Jackson : Classical Electrodynamics cap 14 paragrafo 9.

Un trattamento relativistico e' esposto in:
G.Garibian, Sov. Phys. JETP63 (1958) 1079

Qui faremo una trattazione mooolto qualitativa del processo di emissione, basata su quella del Jackson, Elettrodinamica classica (...ma molto piu' semplice e naive di quella)

Radiazione di transizione

Le caratteristiche principali della RT si possono comprendere qualitativamente senza fare calcoli complicati. Consideriamo il caso di una particella ultrarelativistica con $\gamma >> 1$ che arriva lungo l'asse z dal vuoto (z<0) e penetra in un mezzo con indice di rifrazione n (z>0), la superficie a z = 0 e' quella di separazione dei due mezzi.

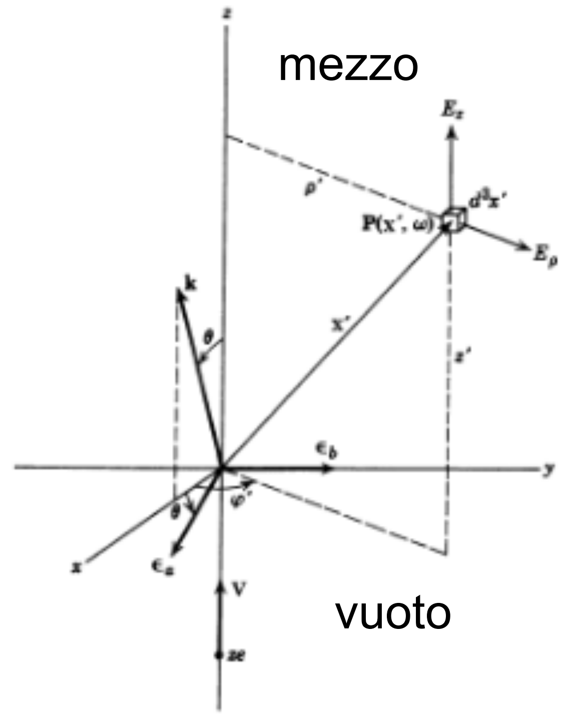

Figure 13.9 A charged particle of charge ze and velocity $\mathbf{v}$ is normally incident along the z axis on a uniform semi-infinite dielectric medium occupying the half-space $z > 0$. The transition radiation is observed at angle θ with respect to the direction of motion of the particle, as specified by the wave vector $\mathbf{k}$ and associated polarization vectors $\boldsymbol{\epsilon}_a$ and $\boldsymbol{\epsilon}_b$.

Radiazione di transizione

a) La distribuzione angolare della radiazione emessa e' confinata in un cono t.c. $\gamma\theta \sim 1$

b) La radiazione di TR e' il risultato dell'interferenza tra il campo della particella incidente e l'onda irraggiata localmente a causa della polarizzazione dipendente dal tempo del mezzo.

Se decomponiamo la corrente in comp. Di fourier, la componente alla freq. ω del campo generato dalla particella ha una componente la cui ampiezza lungo z oscilla come (cfr. cherenkov)

$$\sim \exp(i\omega z/v)$$

La polarizzazione del mezzo emette onde con un'ampiezza che va come

$$\sim \exp(-ikz) = \exp(-i\omega nz/c)$$

Dato che

$$P(\omega,x') \propto E_i(\omega,x'),$$

l'onda emessa va come

$$\sim \exp(i\omega z/v)\exp(-in\omega z/c)$$

$$= \exp(i\omega z(1/v - n/c))$$

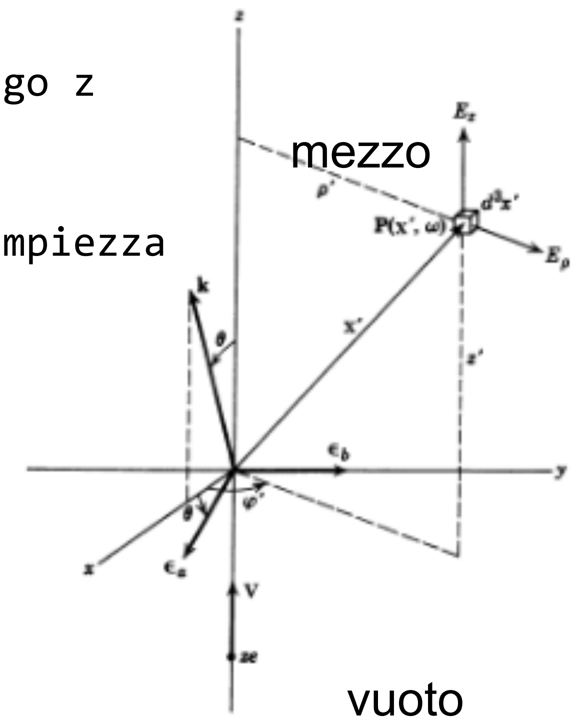

Figure 13.9 A charged particle of charge ze and velocity $\mathbf{v}$ is normally incident along the z axis on a uniform semi-infinite dielectric medium occupying the half-space $z > 0$. The transition radiation is observed at angle θ with respect to the direction of motion of the particle, as specified by the wave vector $\mathbf{k}$ and associated polarization vectors $\boldsymbol{\epsilon}_a$ and $\boldsymbol{\epsilon}_b$.

Radiazione di transizione

Lontano dall'interfaccia fra vuoto e mezzo posta a z = 0, ie per "grandi" z, la fase del campo oscilla rapidamente, l'onda pilota (del campo incidente) e quella della polarizzazione non sono coerenti
→ **<|E|>= 0**, cioe' non c'e' radiazione emessa.
L'unico contributo alla radiazione emessa viene dalla regione in cui la fase del campo non varia apprezzabilmente, cioe' entro uno spessore z t.c.

$$\omega z(1/v - n/c) \lesssim 1$$

Assumendo freq abbastanza alte (sopra la regione ottica, $\omega \gg \omega_p$), la costante dielettrica e puo' essere parametrizzata in funzione di ω come
$\varepsilon/\varepsilon_0 \approx 1 - (\omega_p/\omega)^2$
con ω_p frequenza di plasma del mezzo.
$\boldsymbol{\omega_p = (4\pi N e^2/m)^{1/2} = 1.54\times10^4 N^{1/2} = 28.8(\rho Z/A)^{1/2}}$ **eV,** con N densita' degli e- del mezzo e ρ densita' in gr/cm^3 e Z/A e' il rapporto medio nr atomico e di massa del materiale. Nelle sostanze con densita' dell'ordine dell'unita' $h\omega_p/2\pi \approx 20$ eV, in aria 0.7 eV

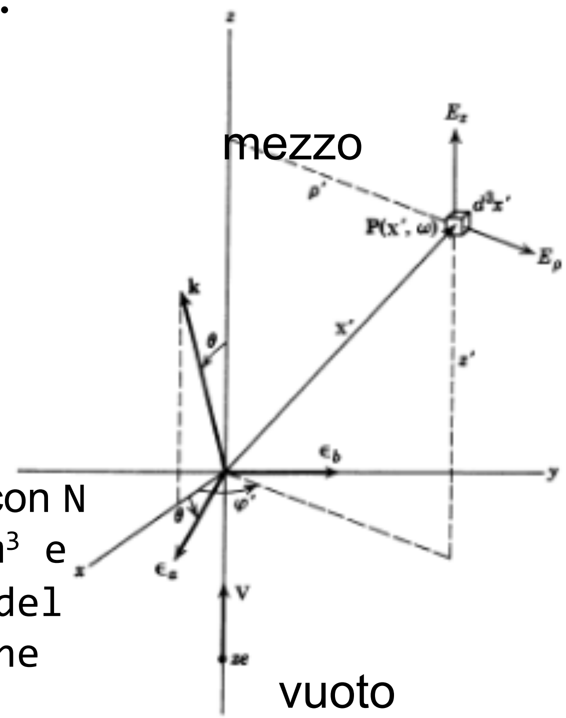

Figure 13.9 A charged particle of charge ze and velocity $\mathbf{v}$ is normally incident along the z axis on a uniform semi-infinite dielectric medium occupying the half-space $z > 0$. The transition radiation is observed at angle θ with respect to the direction of motion of the particle, as specified by the wave vector $\mathbf{k}$ and associated polarization vectors $\boldsymbol{\epsilon}_a$ and $\boldsymbol{\epsilon}_b$.

Radiazione di transizione

$\varepsilon \approx 1 - (\omega_p/\omega)^2$

Nel limite $\omega \gg \omega_p$ $n = (\varepsilon)^{1/2} \approx 1 - (1/2)(\omega_p/\omega)^2$
Per $\beta \approx 1$, $\gamma \approx 1/[2(1-\beta)] \rightarrow 1/\beta = 1 + 1/2\gamma^2$

Sostituisco in $\omega z(1/v - n/c) \lesssim 1$ e ho

$z \sim 2\gamma/\omega_p(\nu + 1/\nu)$ con $\nu = \omega/\gamma\omega_p$
La lunghezza di formazione D, cioe' la profondita' in z della regione da cui la radiazione viene emessa puo' essere definita come il max di $z(\nu)$ (cfr. Jackson).
Il max si ha quando $\nu = 1 \rightarrow$
$D = z(1) = \gamma c/\omega_p$

Per mezzi tipici e per particelle ultrarelativistiche $\gamma \sim 10^3$,
D ~ decine di microns

Radiazione di transizione

L'energia totale emessa nell'attraversare una singola interfaccia e'

$$I = \alpha\gamma h\omega_p/3(2\pi)$$

Qualitativamente il risultato puo' essere ottenuto nel modo seguente: per un osservatore a riposo ad una distanza b dalla traiettoria della particella, il valore max del campo elettrico e' $\mathbf{E = \gamma e/b^2}$ e la durata dell'interazione e' $\mathbf{\Delta t = b/\gamma c}$

Percio' l'energia totale dell'emissione e'

$\mathbf{I \sim E^2 \times \Delta V \sim E^2\, b^2\, c\Delta t = \gamma e^2/b}$

A spanne, il max dell'emissione si ha quando $b = b_{min}$.

Occorre definire b_{min}.

b_{min} e' la lunghezza minima che la particella deve percorrere affinche' il mezzo reagisca al campo E.

L'interazione della particella non avviene con un atomo o un e- singolo, ma con molti atomi vicini alla particella.

Il mezzo puo' essere pensato come un plasma.

Un plasma possiede una frequenza caratteristica ("naturale") che corrisponde alla frequenza tipica di oscillazione elettrostatica in risposta ad una piccola separazione spaziale di carica.

Frequenza di plasma

Per esempio consideramo il caso in cui uno strato di cariche di un solo segno venga spostato dalla posizione quasi-neutra di un tratto infinitesimo δx. Sulla faccia dello strato si sviluppa una densita' di carica $\boldsymbol{\sigma = en\,\delta x}$ e una carica uguale e opposta si sviluppa sulla faccia opposta. In pratica si ha un condensatore a facce piane parallele, in cui si ha un campo
$\boldsymbol{E = -\sigma/\varepsilon_0 = -e\,n\,\delta x/\varepsilon_0}$

Se ora prendiamo una particella fra le due facce, l'equazione del moto dello spostamento δx ci da'
$\boldsymbol{d(\delta x)/dt^2 = eE = -\,e^2 n\,\delta x/m\varepsilon_0 = -\omega_p^2\delta x}$
Il sistema oscilla con la frequenza di plasma.

In risposta ad una sollecitazione esterna, le oscillazioni di plasma verranno osservate solo se la sollecitazione agisce su periodi di tempo > $1/\omega_p$ o su scale di lunghezza > v/ω_p
Nel nostro caso percio' il mezzo non reagisce al campo della particella su scale di lunghezza inferiori a $b_{min} = c/\omega_p$

Radiazione di transizione

$I \sim E^2 \times \Delta V \sim E^2 b^2 c\Delta t = \gamma e^2/b$
Se poniamo b = bmin otteniamo
$I \sim \gamma e^2\omega_p/c = \gamma e^2 h\omega_p/hc = \gamma\alpha h\omega_p$

$$I = \int_0^\infty \frac{dI}{d\nu}\, d\nu = \frac{z^2 e^2 \gamma \omega_p}{3c} = \frac{z^2}{3(137)}\, \gamma\hbar\omega_p \qquad (13.8$$

Lo spettro della radiazione che si ottiene dal calcolo esatto e'

$$\frac{dI}{d\nu} = \frac{z^2 e^2 \gamma \omega_p}{\pi c}\left[(1+2\nu^2)\ln\left(1+\frac{1}{\nu^2}\right) - 2\right]$$

Nel limite di piccoli e grandi ν

$$\frac{dI}{d\nu} \simeq \frac{z^2 e^2 \gamma \omega_p}{\pi c}\begin{cases} 2\ln(1/e\nu), & \nu \ll 1 \\ \frac{1}{6\nu^4}, & \nu \gg 1 \end{cases}$$

Circa il 90% della radiazione emessa e' contenuto nell'intervallo di $0.1 < \nu < 1$.
Per valori tipici $h\omega_p \sim 20$ eV e $\gamma \sim 1000$, l'intervallo di energia dei fotoni emessi e' 2 – 20 keV, cioe' **raggi X** (molli).
Al di sopra di $\nu = 1$ c'e' poca energia emessa

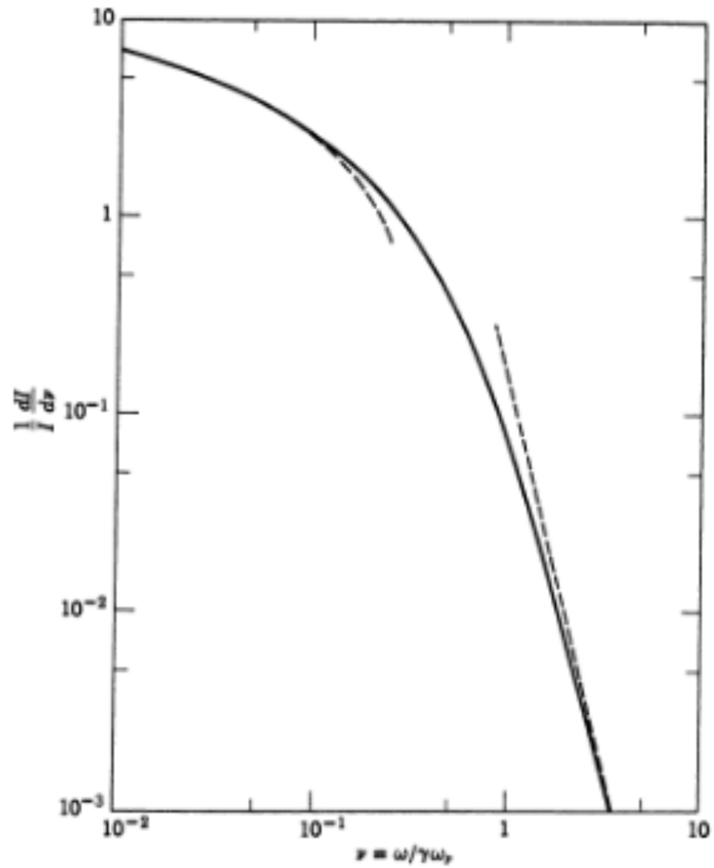

Figure 13.11 Normalized frequency distribution $(1/I)(dI/d\nu)$ of transition radiation as a function of $\nu = \omega/\gamma\omega_p$. The dashed curves are the two approximate expressions in (13.86).

Radiazione di transizione

- L'energia irraggiata ad ogni superfice di separazione e':

$$W = \frac{1}{3}\alpha\hbar\omega_p\gamma \qquad W \propto \gamma = E/m$$

particelle della stessa energia ma massa molto diversa hanno γ molto diversi e quindi emissione diversa → separazione e/p, K/π, e/π,...

- **Il numero di fotoni emessi per superfice di separazione e' piccolo:**

$$N_{ph} \approx \frac{W}{\hbar\omega} \propto \alpha \approx \frac{1}{137}$$

Si ha emissione apprezzabile solo per γ molto alti > 1000 e servono molte interfacce di separazione

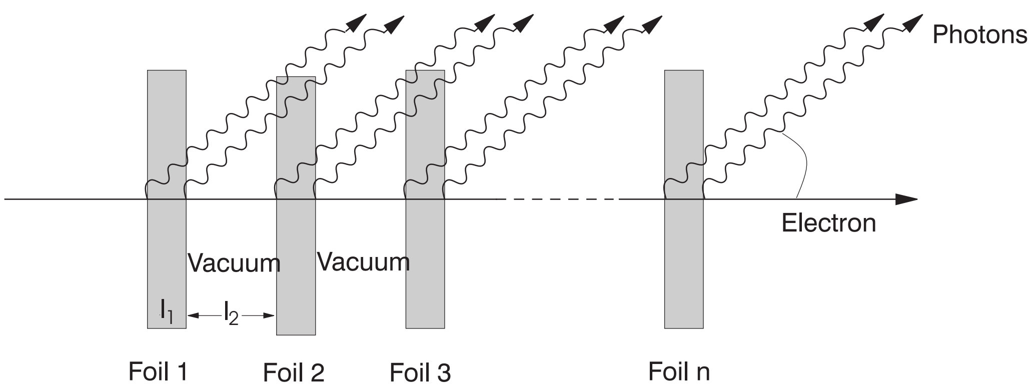

Radiazione di transizione

The observed spectrum is modified for a stack of foils by the absorption characteristics of the foil material. The absorption length decreases rapidly as the photon energy decreases (ie in the soft x-ray range). When the x-ray absorption spectral variation is combined with the basic spectrum from a single foil, the net spectrum will often show a broad peak centered in the soft x-ray range. As the number of foils is increased the spectral peak will shift to higher energies, because the softer x-ray energies will be more strongly absorbed.

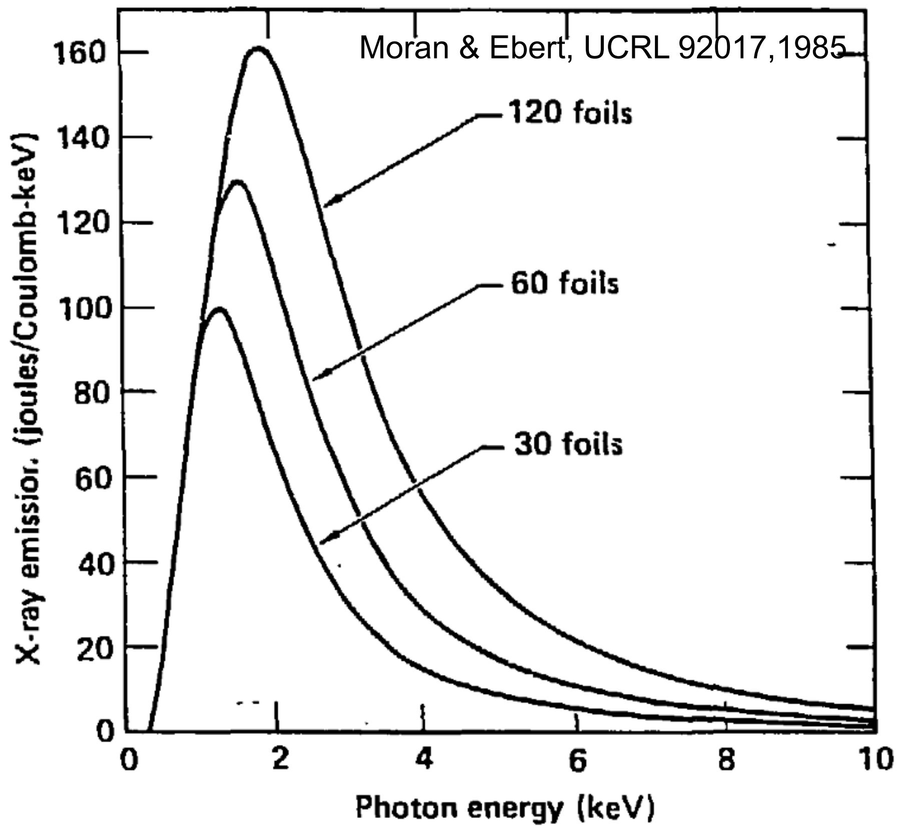

Radiazione di transizione

- I radiatori devono essere a basso Z

  Bisogna evitare di riassorbire I fotoni emessi (vedi in seguito effetto fotoelettrico proporzionale a Z^5).

- Lo spessore dei radiatori deve essere ≥ della lunghezza di formazione D.

$$D = \frac{\gamma c}{\omega_p}$$

Per materiale tipo plastica $\omega_p \sim 30\text{x}10^{15}\ \text{s}^{-1}$ e se $\gamma \sim 1000$

→ D ~ 10 μm, in aria ~ mm

Transition radiation

- Number of emitted photons / boundary is small $N_{ph} \approx \frac{W}{\hbar\omega} \propto \alpha \approx \frac{1}{137}$

  → Need many transitions → build a stack of many thin foils with gas gaps

- Emission spectrum of TR = f(material, γ)

  Typical energy: $\hbar\omega \approx \frac{1}{4}\hbar\omega_p\gamma$

  → photons in the keV range

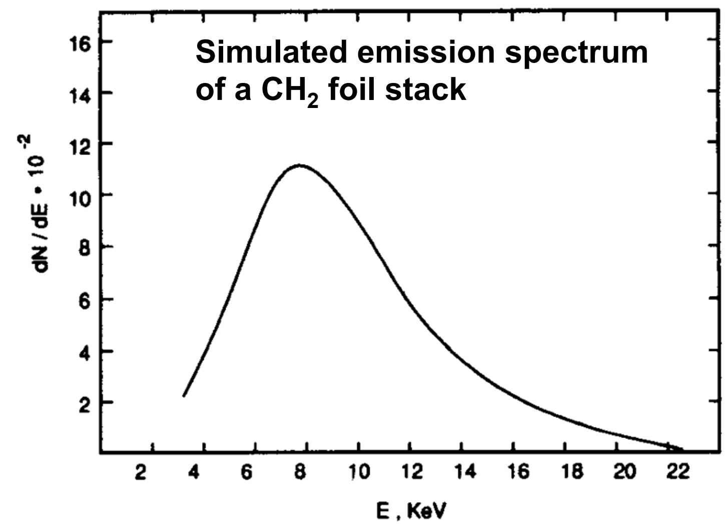

- X-rays are emitted with a sharp maximum at small angles $\theta \propto 1/\gamma$
  → TR stay close to track and the particle loses energy by collisions (ie bethe bloch)→ x-ray photons are not very well separated

  - Particle must traverse a minimum distance, the so-called formation zone Z_f, in order to efficiently emit TR. $Z_f = \frac{2c}{\omega(\gamma^{-2} + \theta^2 + \xi^2)}, \quad \xi = \omega_p / \omega$

Z_f depends on the material (ω_p), TR frequency (ω) and on γ.
Z_f (air) ~ mm, Z_f (CH_2) ~ 20 μm →
important consequences for design of TR radiator.

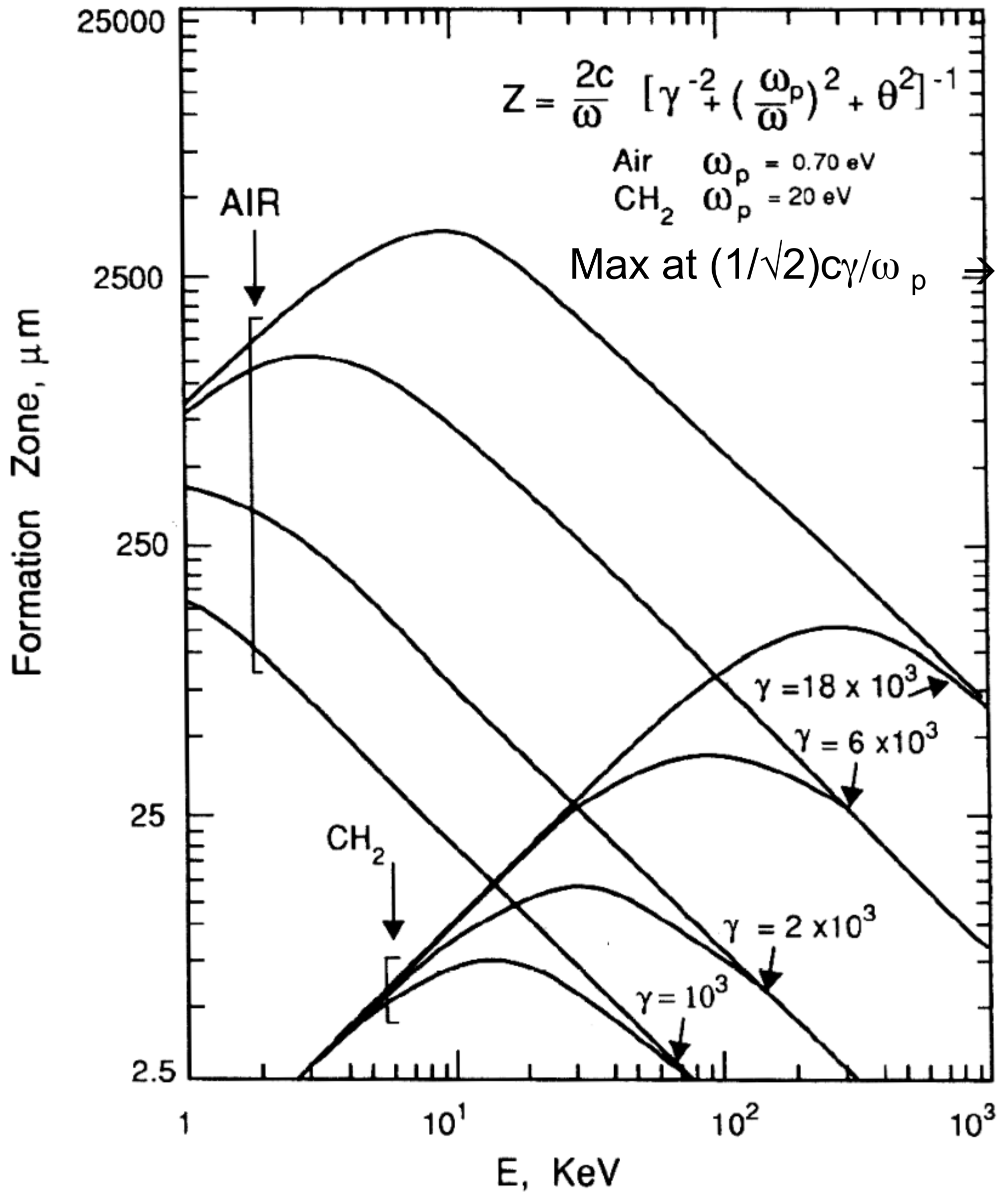

$$Z = \frac{2c}{\omega}\left[\gamma^{-2} + \left(\frac{\omega_p}{\omega}\right)^2 + \theta^2\right]^{-1}$$

Max at $(1/\sqrt{2})c\gamma/\omega_p$ → NB: e' valore stimato con i "calcoli" di prima

Length of formation zone for different γ and as function of ω (E = ω)

High ω for CH_2:
$\gamma^{-2} >> (\omega_p/\omega)^2$:
formation zone length for air and CH_2 about equal, but $\omega > \gamma\omega_p$, i.e. almost no yield

φ *in equations corresponds to θ in figure*

From: B. Dolgoshein, "Transition Radiation Detectors", NIM A326(1993)434-469